Marine and Petroleum Geology 132 (2021) 105204

Contents lists available at ScienceDirect

Marine and Petroleum Geology

journal homepage: www.elsevier.com/locate/marpetgeo

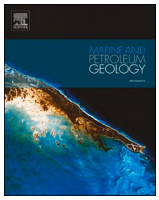

U–Pb dating of carbonate veins constraining timing of beef growth and oil generation within Vaca Muerta Formation and compression history in the Neuquén Basin along the Andean fold and thrust belt

David Cruset [a,*], Jaume Vergés [a], Nuno Rodrigues [b], Jorge Belenguer [a], Enric Pascual-Cebrian [a], Ylènia Almar [a], Irene Pérez-Cáceres [a], Chiara Macchiavelli [a], Anna Travé [c], Aratz Beranoaguirre [d,e,f], Richard Albert [e,f], Axel Gerdes [e,f], Grégoire Messager [b]

[a] Group of Dynamics of the Lithosphere (GDL). Geosciences Barcelona (Geo3Bcn-CSIC), Barcelona, Spain
[b] EQUINOR ASA, Exploration Research, Norway
[c] Departament de Mineralogia, Petrologia i Geologia Aplicada, Facultat de Ciències de la Terra, Universitat de Barcelona (UB), Barcelona, Spain
[d] Geologia Saila, Euskal Herriko Unibertsitatea UPV/EHU, Bilbao, Spain
[e] Department of Geosciences, Goethe-University Frankfurt, Frankfurt am Main, Germany
[f] Frankfurt Isotope and Element Research Center (FIERCE), Goethe-University Frankfurt, Frankfurt am Main, Germany

ARTICLE INFO

Keywords:
U-Pb dating
Calcite and dolomite cements
Fracture history
Neuquén basin
Andean compression

ABSTRACT

We combine structural analysis of fractures with 22 U–Pb dates measured in fracture-filling carbonate cements from bed-parallel fibrous calcite veins (beef), conjugated veins and faults within the Vaca Muerta Formation along the Andean fold and thrust belt in the Neuquén Basin. The measured ages constrain accurately the relationships between overpressures caused by hydrocarbon generation and Andean compression as mechanisms for natural fracturing and vein formation.

Two generations of fibres have been identified in beef. The first one, consists of dark fibres from the inner zones, which are perpendicular to bedding and contain abundant cone-in-cone structures and hydrocarbon inclusions. U–Pb dating of these fibres yielded Early to Late Cretaceous ages from 116.7 ± 17.7 to 78.8 ± 10.2 Ma. The second generation of fibres corresponds to the outer zones and consists of white fibres oblique to bedding, indicating growth during layer-parallel shortening.

Bed-perpendicular veins cutting beef yielded Late Cretaceous-late Palaeocene dates from 72.8 ± 22.4 to 60.9 ± 10.4 Ma. Eocene ages from 52.0 ± 2.9 to 42.2 ± 18.9 Ma were measured in bed-parallel slip surfaces and reverse and strike-slip faults, whereas Miocene dates from 13.9 ± 2.6 to 6.2 ± 1.1 Ma were measured in E-W calcite veins.

U–Pb dating of veins, structural analysis of fractures and subsidence curves, indicate that beef inner zones formed in the oil window during burial of the Neuquén basin, and that tectonic stresses could enhance their formation. Beef outer zones and bed-perpendicular veins formed during E-W Late Cretaceous-late Palaeocene layer-parallel shortening. Contrarily, late Palaeocene-late Eocene bed-parallel slip surfaces and faults and Miocene E-W veins formed during NE-SW and E-W syn-to post-folding deformation, respectively. In both cases, syn-to post-folding compression occurred synchronously with forelandward migration of magmatic activity attributed to flat subduction of the Pacific slab beneath the Andes.

* Corresponding author.
E-mail addresses: dcruset@geo3bcn.csic.es (D. Cruset), jverges@geo3bcn.csic.es (J. Vergés), nunr@equinor.com (N. Rodrigues), jbelenguer83@gmail.com (J. Belenguer), enricpascu@gmail.com (E. Pascual-Cebrian), yleniaalmar@yahoo.es (Y. Almar), irepcaceres@gmail.com (I. Pérez-Cáceres), chiaramacchiavelli13@gmail.com (C. Macchiavelli), atrave@ub.edu (A. Travé), aratz.beranoaguirre@ehu.eus (A. Beranoaguirre), albertroper@em.uni-frankfurt.de (R. Albert), gerdes@em.uni-frankfurt.de (A. Gerdes), gmess@equinor.com (G. Messager).

https://doi.org/10.1016/j.marpetgeo.2021.105204
Received 27 March 2021; Received in revised form 14 June 2021; Accepted 26 June 2021
Available online 29 June 2021

1. Introduction

Tectonic deformation has high impact on fluid systems within sedimentary basins, creating migration paths through fracturing and triggering fluid migration through the development of fluid overpressures (Ge and Garven, 1989; Machel and Cavell, 1999; Bitzer et al., 2001; Roure et al., 2005; Cosgrove, 2015; Zanella et al., 2015). Deciphering the link between migration of fluids and the tectonic history of sedimentary basins requires to stablish the correct chronology of fracturing and fluid flow events, integrating structural analyses and dating methods applied to syn-kinematic minerals precipitated in fractures. In recent years, significant advances have been made to constrain the absolute timing of fluid migration and fracturing. One of the more effective geochronological methods is the U–Pb dating of carbonates using laser ablation-inductively coupled plasma-mass spectrometry (e.g., Roberts and Walker, 2016). As some examples, recent works about the application of this dating method together with fracture structural analyses have been focused on to constrain the absolute age and sequence of deformation in the compressional Oman Mountains, SE Pyrenees and Bighorn basin as well as the extensional Viking graben and Red Sea (Roberts and Walker, 2016; Nuriel et al., 2017; Hansman et al., 2018; Beaudoin et al., 2018; Cruset et al., 2020). Additionally, U–Pb dating of carbonates has also been used to decipher the diagenetic history and the timing of hydrocarbon migration in sedimentary basins (e.g., Paris basin: Mangenot et al., 2018; Pagel et al., 2018; Namibe basin: Rochelle-Bates et al., 2020; Zanella et al., 2021).

Bedding-parallel fibrous veins, also called "beef" due to their texture, are common in many sedimentary basins worldwide (e.g., Cobbold et al., 2013). These veins are of special interest since they have a direct relationship with overpressures and natural hydraulic fracturing due to oil, gas and solid hydrocarbons generation (Stoneley, 1983; Cobbold and Rodrigues, 2007; Rodrigues et al., 2009; Zanella et al., 2014). However, the potential influence of tectonic stresses during beef growth is still under discussion since very few studies provide absolute time constrains of their formation linked to compressional deformation in sedimentary basins hosting these veins (Zanella et al., 2021). Furthermore, the timing of formation of these veins has only been inferred using indirect methods such as the integration of structural analysis with cross-cutting relationships between veins and dated igneous intrusions, growth strata and tectonostratigraphic constrains, burial curves and maturity estimations (e.g., Rodrigues et al., 2009; Ukar et al., 2020).

The Neuquén Basin, the most prolific hydrocarbon province of Argentina, has world class exposures of veins within or associated with its main source rock, the basinal black shales of the Tithonian-early Valanginian Vaca Muerta Formation (e.g., Weaver, 1931; Urien and Zambrano, 1994; Cruz et al., 1996). The veins within the Vaca Muerta Formation occur in outcrops along the Andean fold and thrust belt and consist of: 1) bitumen veins (Cobbold et al., 1999, 2014, 2014; Zanella et al., 2015); 2) beef (Rodrigues et al., 2009; Zanella et al., 2015; Ukar et al., 2017a); and 3) bed-perpendicular conjugate sets of veins (Ukar et al., 2017b).

Bedding-parallel fibrous veins (Beef) within the Vaca Muerta Formation occur within the most organic rich beds and are constituted of two generations of calcite related to successive episodes of hydrofracturing (Ukar et al., 2017a; Rodrigues et al., 2009; Ravier et al., 2020; Larmier, 2020; Larmier et al., 2021). Typically, the first generation consists of the inner zones of beef, which are formed of fibres that grew perpendicular to bedding and to the median suture, contain abundant bitumen inclusions and hydrocarbon-bearing fluid inclusions giving a dark colour to the inner zone of the veins. This direct relationship between growth of inner zones along horizontal fractures and hydrocarbons implies lithostatically overpressured pore fluids composed of mixed aqueous and hydrocarbon phases, probably due to chemical compaction during transformation of solid kerogen to oil (Rodrigues et al., 2009), as demonstrated by the sandbox models of Zanella et al. (2014). Rodrigues et al. (2009) estimate that the fibres of the inner zones formed during Aptian and Albian, when the Vaca Muerta Formation was in the oil window period. Contrarily, Ukar et al. (2020), based on subsidence curve analysis combined with clumped isotope temperatures measured in beef (Weger et al., 2019), concluded that they formed from the Cenomanian to the Danian and probably to the Miocene. The second generation of fibres consist of the outer zones of beef, which are formed of multiple stages of vein opening filled with fibres that grew oblique to bedding and have a white colour due to the lack of hydrocarbon inclusions. The obliquity of the fibres indicate that they formed during the early stages of layer-parallel shortening associated to tectonic pulses building the Andes (Rodrigues et al., 2009; Zanella et al., 2015; Ukar et al., 2017a), which occurred during Cenomanian to Campanian when the Vaca Muerta Formation was in the gas window (Rodrigues et al., 2009). Crosscutting the beef, several sets of bed-perpendicular and conjugate veins (some of them filled with carbonate cement) register the evolution of folding during the Andean compression (Ukar et al., 2017a, b).

Previous estimates on both the timing of beef growth and of younger fractures in the Neuquén Basin are based on indirect methods such as crosscutting relationships between beefs and volcanic rocks dated by radiometric methods and subsidence curve analysis (e.g., Rodrigues et al., 2009; Ukar et al., 2020). To refine these cross-cutting ages we present absolute ages for the beef growing coevally with oil generation as well as subsequent conjugated vein systems and faults developed during the different stages of Andean compression. To reach this goal, we use U–Pb dating applied to fracture-filling calcite and ankerite from beef, E-W, ENE-WSW and WNW-ESE trending conjugated veins, bed-parallel slip surfaces, strike-slip and reverse faults. Ages are obtained from 27 samples collected within fractures in the Tithonian to Valanginian basinal marls of the Vaca Muerta Formation and Hauterivian limestones of the Agrio Formation along the Agrio, Chos Malal and Malargüe fold and thrust belts. The results allow to constrain the absolute age of beef growth, oil generation and later fractures as well as the potential influence of tectonic stresses related to the Andean compression on beef growth.

2. Geology of the Neuquén Basin

The Neuquén Basin in northern Patagonia is the result of the complex tectonic history of the western margin of Gondwana (Fig. 1A), and registers a sedimentary record from the Carboniferous to the Quaternary (Howell et al., 2005; Mosquera and Ramos, 2006; Rojas Vera et al., 2015, Fig. 1B).

The oldest rocks of the basement consist of a succession of up to 2700 m of Carboniferous marine shales from the Andacollo Group, which were deformed during the Gondwanian orogeny (Hervé et al., 2013). This succession was unconformably overlain by up to 2000 m of Permian to Triassic volcanic and sedimentary deposits from the Choiyoi Group (Stipanicic et al., 1968; Sagripanti et al., 2015; Horton et al., 2016). Younger rocks consist of the Late Triassic to Early Jurassic succession of non-marine deposits and volcanic sequences of the Pre-Cuyo unit (Gulisano, 1981). This unit has a variable thickness from 50 to 3000 m and deposited during extensional tectonics (Gulisano and Gutiérrez-Pliemling, 1995; Sagripanti et al., 2015).

Above the Pre-Cuyo unit, the transgression of the Pacific Ocean resulted in the deposition of distal shales, turbidites, platform sandstones and distal fluvial deposits of the Cuyo Group during the Early to Middle Jurassic (Gulisano, 1981; Zavala, 1996; González-Estebenet et al., 2021). During this period, the subduction of the proto-Pacific oceanic crust below western Gondwana began, and a back-arc basin developed (Howell et al., 2005). This subduction period continued during the Late Jurassic to the Early Cretaceous, when successive transgressive-regressive thick successions deposited in the back-arc basin and rift-fault blocks were locally uplifted (Cobbold and Rossello, 2003; Mosquera and Ramos, 2006; Zamora Valcarce et al., 2006). Older deposits are Middle-Late Jurassic in age, and are represented by the

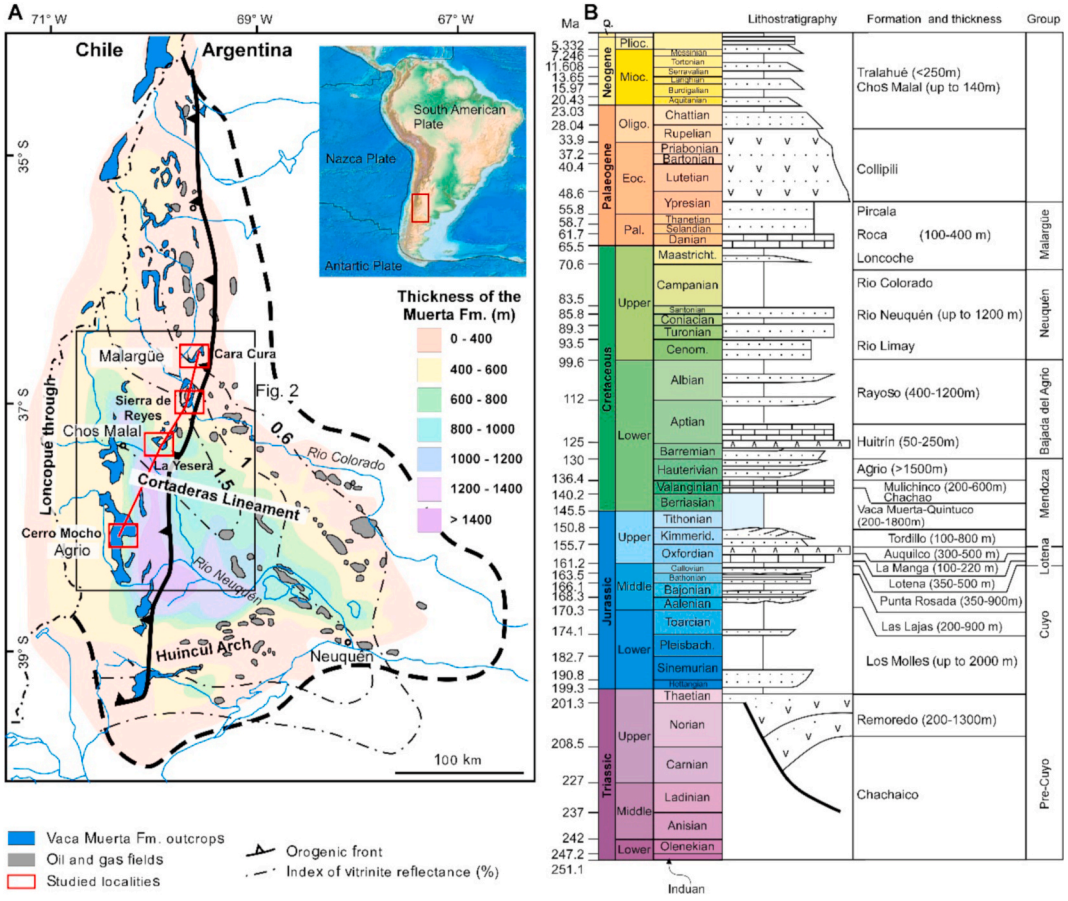

Fig. 1. Thickness map of Vaca Muerta Formation based on Cobbold et al. (1999) showing the oil and gas fields and vitrinite reflectance values of the Vaca Muerta Formation. The outcrops of the Vaca Muerta Formation, its thickness based on Domínguez et al. (2020), the location of the studied areas (red boxes) and of Fig. 2 (black box) are also shown. The red line indicates the location of the cross-section in C. B) Stratigraphy of the Neuquén Basin. Thicknesses of the depositional groups are based on: Pre-Cuyo (Carbone et al., 2011), Cuyo (Arregui et al., 2011a), Lotena (Arregui et al., 2011b), Mendoza (Leanza et al., 2011; Schwarz et al., 2011; Spalletti et al., 2011a, b; Domínguez et al., 2020), Bajada del Agrio (Gutierrez-Pleimling et al., 2011; Zavala and Ponce, 2011), Neuquén (Garrido, 2011) and Malargüe (Rodríguez, 2011). The thickness of the Chos Malal and Tralahué Formations are based on Cervera and Leanza (2009) and Ramos (1998a), respectively. (For interpretation of the references to colour in this figure legend, the reader is referred to the Web version of this article.)

transgressive/regressive successions of the marine to non-marine sandstones of the Lotena Formation, La Manga limestones and sandstones and the Auquilco gypsums (Legarreta and Gulisano, 1989; Gulisano and Gutiérrez-Pliemling, 1995; Veiga et al., 2011). The Auquilco Formation is unconformably overlain by the fluvial sandstones of the Kimmeridgian-Tithonian Tordillo Formation, which represents the base of the Mendoza Group (Leanza et al., 1977; Gulisano and Gutiérrez--Pliemling, 1995; Veiga and Spalletti, 2007). This formation has a maximum depositional age of 153–151 Ma, according to detrital zircon U–Pb data (Naipauer et al., 2012). Above the Tordillo Formation, the early Tithonian to early Valanginian Vaca Muerta-Quintuco system developed, which consist of dark basinal marls and shallower mixed platforms related to a marine transgression of the Palaeo-Pacific (Riccardi et al., 2000; Kietzmann et al., 2015; Iglesia Llanos et al., 2017; Martínez et al., 2018).

Overlying the Vaca Muerta-Quintuco system, the younger units of the Mendoza group are represented by the regressive proximal marine deposits of the Valanginian Mulichinco Formation and the transgressive organic-rich marine sediments of the Valanginian-Hauterivian Agrio Formation (Schwarz et al., 2006; Aguirre-Urreta et al., 2017). Over these rocks, the evaporites of the Huitrín Formation and fluvial and lacustrine sediments of the Rayoso Formation deposited from the Barremian to the end of the Albian, representing the last incursion of the Pacific Ocean in the Neuquén Basin (Leanza, 2003).

From the late Early Cretaceous, the Neuquén Basin was affected by regional inversion and fold and thrust belt development in the eastern side of the Andes (Cobbold and Rosello, 2003; Zamora Valcarce, 2006; Rojas Vera et al., 2015). This compressional deformation was divided into three tectonic phases: The first one occurred from the Aptian to Late Cretaceous (Peruvian), the second one during the Eocene (Incaic) and the last phase during the Miocene to present day (Quechua) (Steinmann, 1929; Cobbold and Rosello, 2003). During the late Early Cretaceous Peruvian phase, continental foreland deposits of the Neuquén Group deposited at the thrust front. The base of the Neuquén group is dated at around 99 Ma and is separated from underlying rocks through a regional angular unconformity (Tunik et al., 2010). This continental deposition was followed by the Campanian to Early Eocene Malargüe Group, which represents an Atlantic transgression in the Andean foreland basin (Barrio, 1990; Aguirre-Urreta et al., 2011). Coevally with Late Cretaceous compression and uplift, volcanic and intrusive rocks occurred along the eastern Andes from 100 Ma to 61 Ma (Zamora Valcarce et al., 2006; Rodrigues et al., 2009). Compressional deformation continued during the Eocene Incaic phase, leading to transpression (Cobbold and Rossello, 2003). Eocene deformation was accompanied with the intrusion of the dykes and laccoliths of the Collipilli Formation, which yield middle Eocene ages from 48 to 45 Ma obtained from K–Ar dating of the whole rock (Llambías and Rapela, 1989). The Oligocene and Early Miocene period was characterized by deposition of non-marine sediments in basins such as the Loncopué through, which formed within the hinterland of the Andean zone, bounded by the Loncopué Fault System.

According to Ramos (1978), Llambías and Rapela (1989), Urien and Zambrano (1994) and Folguera et al. (2010) this is a Cenozoic westward dipping normal fault, whereas Lesta et al. (1985) and Cobbold and Rossello (2003) interpret the Loncopué fault system as a Jurassic normal fault reactivated as reverse fault during the Cenozoic. Late Miocene to present Quechua compression in the Neuquén Basin phase is characterized by significant erosion and deposition of continental syn-orogenic sediments (e.g., Tralahué and Chos Malal Formations; Ramos, 1998; Cobbold and Rossello, 2003; Zamora Valcarce et al., 2006; Cervera and Leanza, 2009; Messager et al., 2010; Lebinson et al., 2018). Plio-Quaternary tectonics in the Neuquén Basin is characterized by compression according to Messager et al. (2010). These authors conclude, based on geomorphic studies, that Plio-Quaternary fluvial terraces were the result of the reactivation and concomitant erosion of the Miocene thrust front. Accordingly, the maximum horizontal stress measured in boreholes correlate to the main direction of plate convergence, suggesting regional compression (Guzmán et al., 2007; Colavitto et al., 2019). Contrarily, other authors argue that the more recent tectonic history of the Andes was characterized by extensional tectonics, based on the geochemical study of volcanic rocks and structural analyses reporting the presence of Plio-Quaternary extensional faults and half grabens (Drake, 1976; González-Ferran, 1995; Manceda and Figueroa, 1995; Ramos, 1998; Hildreth et al., 1999; Folguera et al., 2005).

The study area is located at the frontal domain of the Agrio, Chos Malal and Malargüe fold and thrust belts (Fig. 2A). They are characterized by thick-skinned deformation, although superimposed thin-skinned structures detached in the evaporites of the Auquilco and Huitrin Formations and shales of the Vaca Muerta Formation are also observed (Ramos, 1978, 1981, 1981; Cobbold and Rosello, 2003; Folguera et al., 2007; Zamora Valcarce, 2007; Messager et al., 2010; Sánchez et al., 2018). The western sector of the Agrio and Chos Malal fold and thrust belts corresponds to the Loncopué through, whereas they are separated each other by the Cortaderas lineament (Zapata and Folguera, 2005; Zamora Valcarce, 2007).

3. The Vaca Muerta formation

The Vaca Muerta Formation mainly consists of a succession of bituminous black shales, sporadic volcanic deposits and limestones (Weaver, 1931; Leanza et al., 2011; Zeller et al., 2015; Kietzmann et al., 2016), although storm deposits have been identified at the base of the formation (Krim et al., 2017). The Vaca Muerta Formation ranges in age from the early Tithonian to the Valanginian, according to biostratigraphic and palaeomagnetic data (Kietzmann et al., 2015; Iglesia-Llanos et al., 2017; Martínez et al., 2018). A more recent study provides absolute U–Pb dates of Zircons within the Vaca Muerta Formation of 152 to 138.7 Ma, also indicating ages from early Tithotian to Valanginian (Aguirre-Urreta et al., 2019). This formation deposited in an embayment with a NW-SE alignment and is limited to the south by the Huincul Arch (e.g., Leanza and Hugo, 1997; Fernández et al., 2003; Spalletti et al., 2008; Leanza et al., 2011, Fig. 1A). The Vaca Muerta Formation represents the deepest and distalmost part of a largely NW-prograding depositional system formed by the mixed platforms of the Quintuco-Picún Leufú Formation, which represent the shallower deposits of the system. These platforms change basinwards to the Vaca Muerta marls, as perfectly reconstructed by the geometry of carbonate platform clinoforms based on a large seismic and well database (González Tomassini et al., 2016; Domínguez et al., 2020; Zeller et al., 2014, 2015). The beginning of the deposition of the Vaca Muerta Formation was characterized by restricted seawater circulation and euxinic conditions, which evolved rapidly to more oxygenated sedimentation (Krim et al., 2017, 2019, 2019).

The thickness of the Vaca Muerta-Quintuco system shows a high variation along the Neuquén embayment, with up to 1800 m thick at the basin depocenter and between 400 and 200 m at its margins (Domínguez et al., 2020, Fig. 1A). The high variation of the thickness of this system along the Neuquén Basin is also corroborated by several subsidence burial curves of Cruz et al. (1996), Parnell and Carey (1995), and Zapata et al. (1999) and Scasso et al. (2005). According to their results, the Vaca Muerta-Quintuco system reached a maximum burial of around 6000 m along the Andean front of the Agrio fold and thrust belt during the Miocene. Contrarily, this system reached a maximum burial of around 3700 m at the Chos Malal fold and thrust belt during the Late Cretaceous, whereas at Sierra de Vaca Muerta it reached a burial of up to 1500 m during the Early Cretaceous. Over much of the Neuquén Basin, the index of vitrinite reflectance (Ro) of the Vaca Muerta Formation is between 0.6 and 1.5% (Fig. 1A), indicating that this source rock is within the oil window (Urien and Zambrano, 1994), whereas in the internal parts of the Andean fold and thrust belt, Ro is 2% at the base of the Vaca Muerta Marls and 1.2% near the top, within the gas window (Kozlowski et al. 1997, 1998). Around the Huincul Arch, the Vaca Muerta Formation has low degrees of maturity to produce hydrocarbons due to low burial depth present in the area (Cruz et al., 1996; Stinco and Mosquera, 2003; Scasso et al., 2005).

4. Beef within the Vaca Muerta formation

Beef have been observed in organic-rich shales of the three potential source rocks in the Neuquén Basin: 1) Hettangian to Toarcian Los Molles Formation (Cobbold et al., 2013); 2) Tithonian to Valanginian Vaca Muerta Formation (Rodrigues et al., 2009); and 3) Hauterivian Agrio Formation (Cobbold et al., 2013). However, the vast majority of beef are concentrated in the Vaca Muerta black shales.

Beef within the Vaca Muerta Formation are well recognized in outcrops of the Agrio and Chos Malal fold and thrust belts (e.g., Rodrigues et al., 2009; Ukar et al., 2017; Weger et al., 2019), although they are also observed in subsurface cores from the foreland basin (e.g., Ravier et al., 2020). Rodrigues et al. (2009) described, for the first time, the microstructure of beef in detail. These authors concluded that beef are antitaxial veins constituted of a dark inner zone of bed-perpendicular fibres separated by a median suture with wall rock and solid bitumen, and a white outer zone of oblique fibres. A more recent study reported that occasionally, beef also show syntaxial and ataxial growth features, occasionally (Larmier, 2020). In both cases, beef are formed by multiple phases of calcite cement precipitated during successive stages of fracturing (Rodrigues et al., 2009; Ukar et al., 2017a; Larmier, 2020).

Beef formed at temperatures of around 100 °C at Puerta Curaco, according to clumped isotopes measurements (Eberli et al., 2017; Weger et al., 2019). Contrarily, higher fluid inclusion homogenization temperatures of up to 160 °C have been measured in Arroyo Mulichinco, close to the Neuquén Basin depocenter (Rodrigues et al., 2009; Fall et al., 2017). Beef precipitated from local fluids expelled from the adjacent Vaca Muerta Formation (Weger et al., 2019; Ukar et al., 2020), although the influence of hydrothermal and meteoric fluids is scarcely identified (Larmier, 2020).

In the Neuquén Basin, beef occur close to the organic-rich base of the Vaca Muerta Formation (Rodrigues et al., 2009). Larmier et al. (2021) demonstrated that parameters such as the degree of maturity of the source rock and rheological discontinuities between shales, sandstones and volcanic ashes also controlled the development and distribution of beef. These authors observed a correlation between the maturity of the Vaca Muerta Formation and the number and thickness of beef.

5. Methodology

The U–Pb dating of fracture-filling carbonates in the Neuquén Basin was integrated with field work, structural fracture analysis and petrographic observations. In the study area, 36 samples of fracture-filling calcite and ankerite cements were oriented in the field, and the strike and dip of a planar surface of the specimen were measured. From these samples, 27 of them were selected for U–Pb dating. The location of the dated samples as well as images of dating mounds and hand specimens on the field are shown in Table S1 and partially in Fig. 2B.

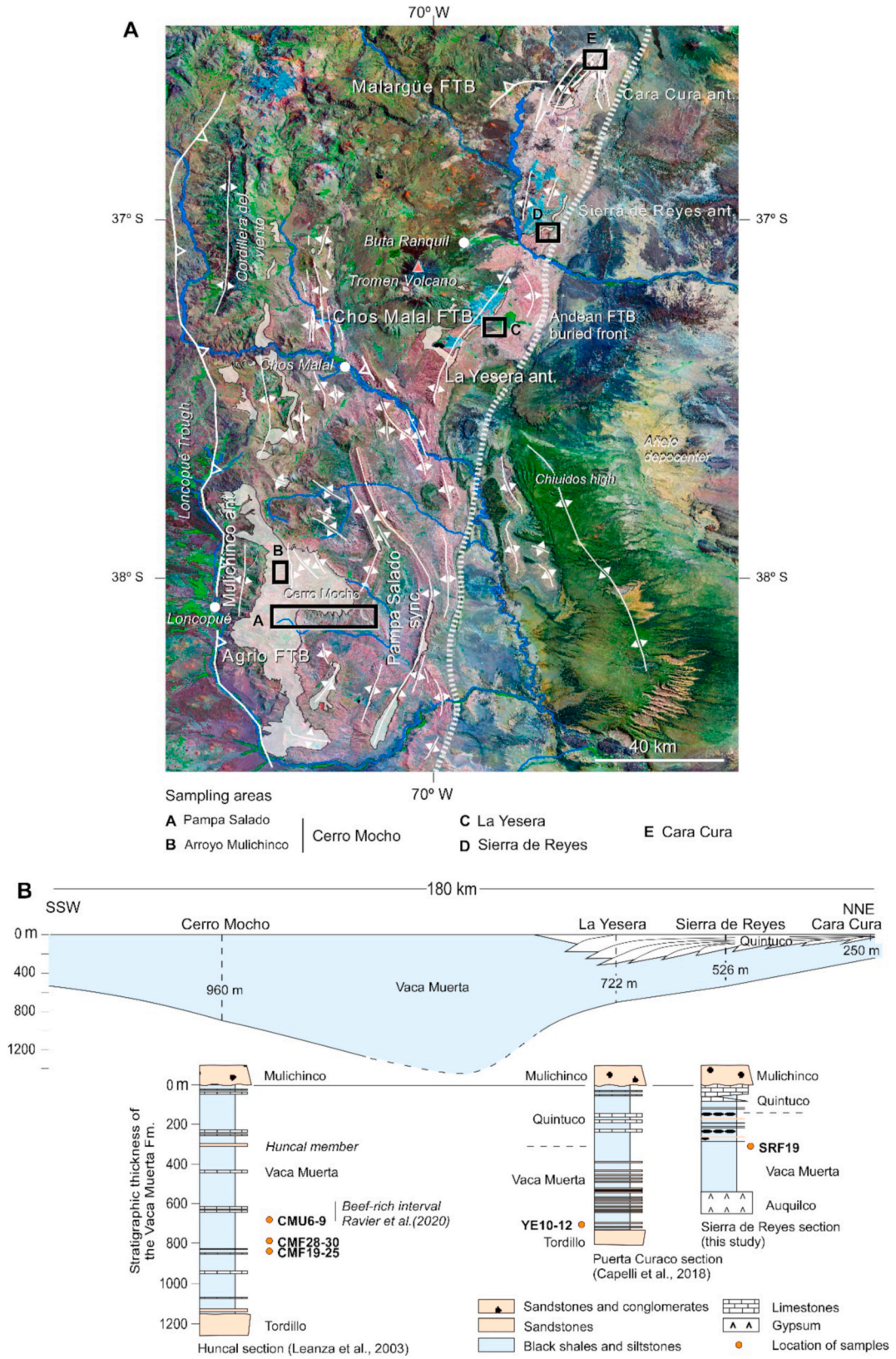

Fig. 2. A) Satellite image showing the study areas (black boxes), main tectonic structures and the Vaca Muerta Formation outcrops (light grey overlay). The position of the buried thrust front is based on the maps of Folguera et al. (2015) and Rojas Vera et al. (2015). The location of this image is shown in Fig. 1A. B) Cross-section showing the thickness of the Vaca-Muerta Formation along the studied areas. The location of beef samples are projected in the stratigraphic cross-sections of Huncal (Cerro Mocho; Leanza et al., 2003), Puerta Curaco (La Yesera; Capelli et al., 2018) and Sierra de Reyes (this work).

Bedding and fracture orientations were measured on the field together with field-based observations on crosscutting relationships between fractures. Later on, each fracture system was plotted in Lower hemisphere Schmidt stereoplots using the program Win-Tensor (v5.8.8.) (Delvaux and Sperner, 2003). The thickness of the Vaca Muerta Formation was estimated from bedding dips measured in the field coupled with remote sensing mapping.

36 polished thin sections from the Vaca Muerta and Agrio host rocks and fracture-filling calcite and ankerite cements were studied by means of optical, cathodoluminescenece and scanning electron microscopy. For scanning electron microscope, a FEI-Quanta 200 device (FEI Europe B. V., Eindhoven, Netherlands) with and EDS Spectrometer (EDAX-Genesis) was used. A CL Technosyn cathodoluminescence device Model 8200 MkII operating at 15–18 kV and 350 μA gun current was used to distinguish the different types of cements.

The U–Pb dating method was previously described in Ring and Gerdes (2016) and Burisch et al. (2017). U–Pb dates were acquired using laser ablation-inductively coupled plasma mass spectrometry (LA-ICPMS) at FIERCE (Frankfurt Isotope and Element Research Center, Goethe University), applying a modified method of Gerdes and Zeh (2006, 2009). A ThermoScientific Element XR sector field ICPMS was coupled to a RESOlution 193 nm ArF excimer laser (COMpexPro 102) equipped with a two-volume ablation cell (Laurin Technic S155). Samples were ablated in a helium atmosphere (300 mL/min) and mixed in the ablation funnel with 1100 mL/min argon and 5 mL/min nitrogen. Signal strength at the ICP-MS was tuned for maximum sensitivity whereas keeping the oxide formation (monitored as $^{248}ThO/^{232}Th$) below 0.2% and low fractionation of the Th/U ratio. Static ablation used a spot size of 193 μm and a fluency of about 2 J/cm^2 at 12 Hz.

Data were acquired in fully automated mode overnight in three sequences of 598 analyses each one. Each analysis consisted of 18 s of background acquisition followed by 18 s of sample ablation and 25 s of washout. During 36 s of data acquisition, the signal of ^{206}Pb, ^{207}Pb, ^{208}Pb, ^{232}Th, and ^{238}U was detected by peak jumping in pulse-counting and analogue mode with a total integration time of ~0.1s, resulting in 360 mass scans. Before analysis, each spot was pre-ablated with 8 laser pulses to remove surface contamination. Soda-lime glass NIST SRM-612 was used as primary reference material (spot size of 50 μm, 8 Hz) together with four carbonate reference materials, which were bracketed in between the analysis of samples.

Raw data were corrected offline using an in-house VBA spreadsheet program (Gerdes and Zeh, 2006, 2009). Following background correction, outliers (±2σ) were rejected based on the time-resolved $^{207}Pb/^{206}Pb$, $^{208}Pb/^{206}Pb$, $^{206}Pb/^{238}U$, and $^{232}Th/^{238}U$ ratios. These ratios were corrected for mass biases and drift over time, using NIST SRM-612. Due to the carbonate matrix, an additional correction was applied (sequence 1: 21.5%, sequence 2: 19.6%, sequence 3: 22.0%), which was determined using WC-1 carbonate reference material (Roberts et al., 2017). It is assumed that no further correction is necessary due to the compositional difference between calcite and ankerite. The $^{206}Pb/^{238}U$ downhole-fractionation during 20s depth profiling was estimated to be 3%, based on the common Pb corrected WC-1 analyses, and was applied as an external correction to all carbonate analyses. Uncertainties for each isotopic ratio are the quadratic addition of the within run precision, counting statistic uncertainties of each isotope, excess of scatter (calculated from NIST SRM-612) and the excess of variance (calculated from WC-1) after drift correction (Horstwood et al., 2016). To account for the long-term reproducibility of the method we added by quadratic addition an expanded uncertainty of 1.5% to the final age of all analysed carbonates. This was deducted from repeated analyses (n = 7) of ASH-15D between 2017 and 2019.

For quality control the following secondary carbonate reference materials were measured. Reference material B6 (41.86 ± 0.53, 42.12 ± 0.88 and 42.72 ± 0.54 Ma; Pagel et al., 2018) was measured in sequences 1, 2 and 3. Reference material ASH-15D (2.907 ± 0.210 Ma; Nuriel et al., 2021) was measured in sequence 1. In addition, a stromatolitic limestone from the Cambrian-Precambrian boundary in South-Namibia (here called NAMA) was analysed during sequence 3 (obtained age of 537.6 ± 10.9 Ma agree with the U/Pb zircon age of 540.1 ± 0.1 Ma from the directly overlying ash layer, Spitskopf formation; Linnemann et al., 2018). Results on the secondary reference materials imply an accuracy and repeatability of the method of about 1.5–2%. Data were displayed in Tera-Wasserburg plots and ages were calculated as lower concordia-curve intercepts using the same algorithms as Isoplot 4.14 (Ludwig, 2012). The ages discussed in this paper are the Tera-Wasserburg intercept ages. All uncertainties are reported at the 2σ level. The analytical results, Concordia graphs and a summary of the U–Pb dating procedure are presented in Table S2.

5.1. Description of sampling areas

Cerro Mocho, La Yesera, Sierra de Reyes and Cara Cura areas were selected for sampling and structural analysis of fractures. La Yesera, Sierra de Reyes and Cara Cura are aligned N–S along the easternmost Andean thrust front, whereas Cerro Mocho is located further west, in a more internal part of the Agrio fold and thrust belt (Fig. 2). These areas show high variations in the thickness of the Vaca Muerta Formation (Fig. 1), allowing to decipher if differences in burial conditions affected the timing of beef formation. Furthermore, Cerro Mocho and La Yesera have been studied by Leanza et al. (2003), Ukar et al. (2017a, b), Weger et al. (2019) and Ravier et al. (2020), providing accurate constrains of their stratigraphy and fracture patterns. The locations of the sampled beef have been projected in the stratigraphic cross sections of Huncal in Cerro Mocho (Leanza et al., 2003), Puerta Curaco in La Yesera (Capelli et al., 2018) and Sierra de Reyes (Fig. 2). To do this projection, bedding orientations and dips measured in the field have been used to calculate the thickness of the Vaca Muerta Formation (Fig. 2B).

The detailed stratigraphy of Cerro Mocho has been studied by Leanza et al. (2003). These authors indicate that the thickness of the Vaca Muerta Formation reaches 1150 m (Fig. 2B). The lack of continuous outcrops and the folding of the Vaca Muerta succession in various anticlines and synclines makes it more difficult to pinpoint the exact location of the beef samples. These beef have been collected in two localities (1 and 2) and they are situated between 300 and 550 m above the bottom of the Vaca Muerta Formation. Localities 1 and 2, show excellent exposures of crosscutting relationships between different types of fractures. The uppermost CMU6-9 beef samples from Locality 1 correspond to the beef-rich interval studied by Ravier et al. (2020), located at about 250 m beneath the turbidites of the Huncal Member described by Leanza et al. (2003) (Fig. 2B). This beef-rich interval has been already characterized from a fracture analysis approach by Ukar et al. (2017a, b) at Arroyo Mulichinco (Fig. 2A). Locality 1 is at the eastern flank of Mulichinco anticline, 13 km to the NE of Loncopué village. In this area, the Vaca Muerta beds dip gently between 20 and 18° towards the SE. Locality 2 is at 17 km to the E of Loncopué village, between the Cerro Mocho anticline and the western limb of the Pampa del Salado syncline. In this area, a system of vertical E-W basaltic dykes cuts the Agrio Formation, whose bedding dips between 10° and 30° to the NW. This system of volcanic dykes has been dated using Ar–Ar geochronology by Zamora Valcarce et al. (2006), yielding an age of 100 Ma (Upper Albian-Cenomanian). At the contact between the Agrio Formation and the volcanic dykes, strike-slip striae sets have been identified after their restoration with respect to bedding. At Locality 2 (Pampa Salado in Fig. 2A), the general structure consists of a fold system affecting the Vaca Muerta Formation, which dips between 16 and 80° towards the ENE and SSW. In this area, the Vaca Muerta Formation contains beef cut by conjugated veins, reverse, normal and strike-slip faults. La Yesera is located at the western limb of La Yesera anticline, 35 km to the ENE of Chos Malal village, and 10 km to the north of the Puerta Curaco stratigraphic section of Weger et al. (2017) and Capelli et al. (2018). In this section, the Vaca Muerta-Quintuco system has a total thickness of around 720 m (Fig. 2B). The studied sector of La Yesera

corresponds to the contact between de Auquilco and Tordillo Formations, and the bottom of the Vaca Muerta Formation, which is much thinner than in Cerro Mocho, with an estimated thickness of 412 m. In this area, sampled beef are located at the bottom of the Vaca Muerta Formation (Fig. 2B) In La Yesera, bedding dips between 45 and 63° to the SE.

The Sierra de Reyes outcrop is located at the southern periclinal termination of the Sierra de Reyes anticline, 15 km to the ENE of Buta Ranquil village (Fig. 2). In this area, the Vaca Muerta-Quintuco system dips between 15 and 20° to the S, has an estimated thickness of 526 m, lies directly above the anhydrite of the Oxfordian Auquilco Formation and passes upwards to the Valanginian Chachao and Mulichinco Formations. The sampled beef in the La Yesera is located in the middle part of the Vaca Muerta Formation (Fig. 2B).

The Sierra de Cara Cura outcrop is at the NE sector of the Sierra de Cara Cura anticline, 62 km to the NE of Buta Ranquil village (Fig. 2). In this area, a N–S thrust emplaces Pre-Cuyo Group above the Agrio Formation, defining a complex fault zone. In the hangingwall, the Pre-Cuyo sequence is uncomfortably overlain by the Vaca Muerta Formation, which is affected by metre-scale reverse faults and intruded by several km-scale sills along the bedding at different levels. In the footwall, the Agrio Formation is also intruded by sills that are folded and thrusted, thus indicating that deformation occurred after their emplacement. In Cara Cura, the Vaca Muerta Formation is involved in reverse faulting and therefore, has not been possible to estimate its thickness. Furthermore, due to the presence of volcanic dykes and sills cutting the Vaca Muerta Formation, the Cara Cura area has been ruled out for U–Pb dating of calcite beef to avoid potential recrystallization of these veins during contact metamorphism.

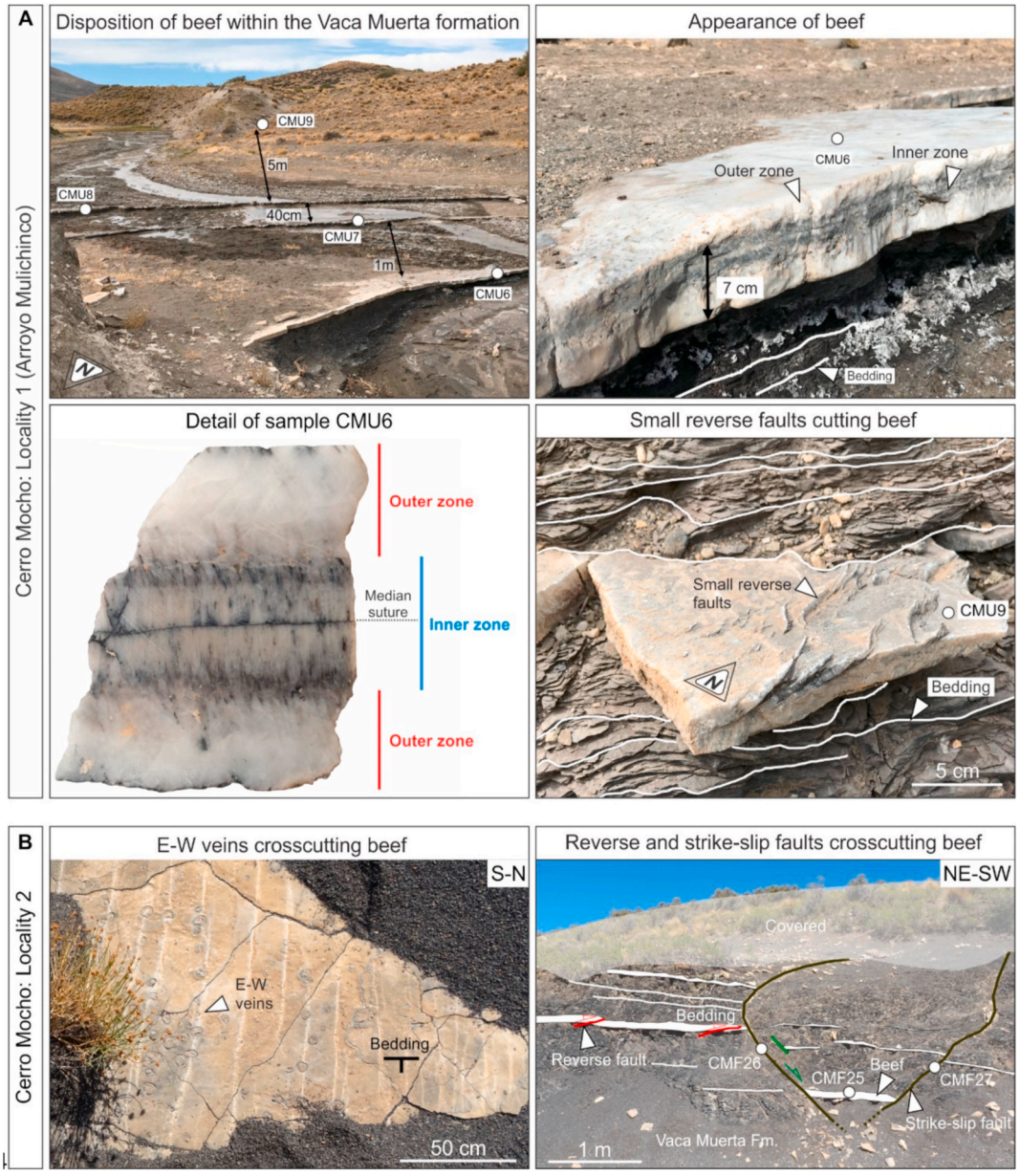

Fig. 3. Field images of beef in Cerro Mocho. The white circles indicate the location of samples. A) Beef interbedded between the Vaca Muerta Formation at Arroyo Mulichinco (Locality 1). Detail of sample CMU6 showing the characteristic inner and outer zone of beef and their crosscutting relationships with small SW-directed thrusts. B) Crosscutting relationships between beef and E-W veins as well as reverse and strike-slip faults at Locality 2 of Cerro Mocho.

6. Sampled beef

6.1. Field observations of beef

Beef have been sampled at Cerro Mocho, La Yesera and Sierra de Reyes and are found in the basal part of the Vaca Muerta Formation. At Cerro Mocho, beef from Locality 1 are in the middle part of the outcropping section of the Vaca Muerta Formation at Arroyo Mulichinco (Fig. 2B). Beef are 2–7 cm thick and with a spacing between veins of 0.4–1 m (Figs. 2B and 3A). In this area, four calcite beef have been sampled and three U–Pb dates have been obtained for their inner zones and one for the outer zones. Beef sampled in Locality 2 are at the lowermost 450 m of the outcropping section of Vaca Muerta Formation and have thicknesses from 1 to 15 cm and are separated each other by distances from 50 cm to 2 m (Figs. 2B and 3B). In this area, beef occasionally form en-échelon vein arrays, have lengths of hundreds of metres and pinch out laterally, sometimes overlapping other beef. At locality 2, eleven calcite beef have been sampled yielding two U–Pb dates from inner zones. In the outer zones U–Pb dating failed.

In La Yesera and Sierra de Reyes, beef are scarcer and thinner than those in Cerro Mocho. In La Yesera (Fig. 4A), beef have a thickness of 5 mm to 3 cm and a width of few centimetres to several metres. In this area, beef occasionally form en-échelon vein arrays, are often cut by E-W bed-perpendicular veins and interbedded with carbonate nodules nucleating from ammonites. In La Yesera, they have been sampled at the bottom of the Vaca Muerta Formation, which has a thickness of 412 m in the study area (Fig. 2B). The three sampled beef are at 50 cm to 1 m of distance each other and have a thickness of 1.5–3 cm. For these samples, only one date has been obtained in the inner zones, whereas U–Pb dating in the outer zones failed. In the studied sector of Sierra de Reyes (Fig. 4B), calcite beef are at basal Vaca Muerta Formation. They are scarce and thin (1–2 cm) and U–Pb dating failed in one measured sample.

6.2. Microstructure of beef

According to optical and scanning electron microscope observations, the sampled beef are constituted of calcite cement with accessory quartz, pyrite and barite. In general, they are constituted of a dark inner zone containing hydrocarbons and shale inclusions and a white outer zone. Occasionally, some beef from Cerro Mocho are only composed of white calcite fibres perpendicular to bedding without a median suture (as defined by Durney and Ramsay, 1973), whereas in other samples the inner zone is almost absent.

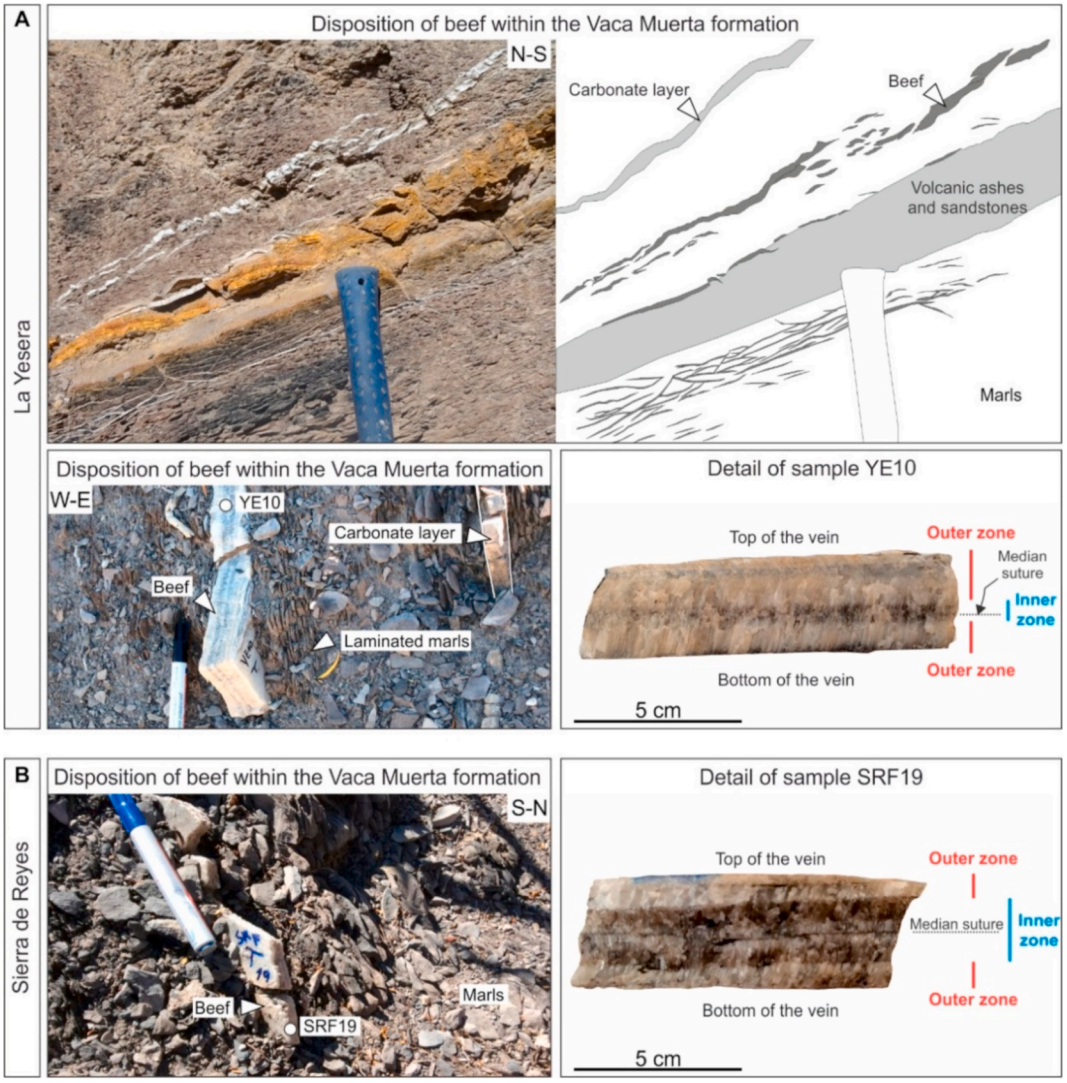

Fig. 4. Field images of beef at La Yesera and Sierra de Reyes. The white circles indicate the location of samples. A) Beef interbedded between the Vaca Muerta Formation at La Yesera. Below is shown the disposition and detail of sample YE10 within the Vaca Muerta Formation at La Yesera. B) Disposition and detail of sample SRF19 within the Vaca Muerta Formation at Sierra de Reyes.

Dark calcite from inner zones of beef contains from 20 to 40 μm width and 250 μm to 1 cm long fibrous calcite crystals arranged perpendicular to fracture walls. Inner zones are divided by a median suture, which contain host rock inclusions (Fig. 5A and B). At Cerro Mocho and Sierra de Reyes, the median suture is located at the centre of beef, whereas for samples from La Yesera it is occasionally located close to their bottom. In both cases, the presence of the median suture, together with the absence of inner zones directly in contact with the host rock, suggest an antitaxial growth of beef as reported by Rodrigues et al. (2009). Close to the median suture, v-shaped host rock trails are often observed (Fig. 5C). These inclusions correspond to the cone-in-cone structures already described by Rodrigues et al. (2009) in calcite beef from the Neuquén Basin, suggesting that they could have formed as consequence of stacking of multiple beef. In the inner zone of beef, it is common to observe inclusions of solid bitumen, indicating a clear relationship between fracture growth and oil generation (Fig. 5D).

White calcite from the outer zone of beef displays from 50 μm to 2 mm width and 1.5 mm to 1 cm long elongated fibres oblique to fracture walls. Occasionally, the outer zones of beef also contain repetitive host-rock trails parallel to the median suture, thus indicating that they formed by crack-seal mechanism (Fig. 5B). Calcite crystals in the outer zones of beef grow in optical continuity with those of the inner zones and display angles of from 50 to 90° with respect to the median suture (Fig. 5A and B). The angular relationship between these crystals and those from the inner zones and the median suture, defines monoclinic and orthorhombic symmetries, as described previously by Rodrigues et al. (2009). Most of the studied beef have a monoclinic symmetry, whereas orthorhombic beef are less frequent. In both cases, the disposition of oblique calcite fibres indicates in general an E-W and NE-SW direction of shortening after their restoration to the horizontal, although SW and WNW directions also have been measured at Cerro Mocho (Fig. 5E).

7. Conjugate vein systems

In the studied areas of the Neuquén Basin, two types of conjugate vein systems postdating beef have been sampled for U–Pb dating: 1) E-W, ENE-WSW and WNW-ESE conjugated veins; and 2) N–S, NNE-SSW and NNW-SSE conjugated veins. The sequence of fracturing based on crosscutting relationships between each fracture system and their dip and orientation with respect to bedding as well as the orientation of each fracture type are shown in Figs. 6 and 7, respectively.

7.1. Field observations of conjugated veins

The E-W, ENE-WSW and WNW-ESE conjugated veins have openings of up to 5 mm, and very occasionally up to 10 cm, have lengths from few cm to 1 m and are locally arranged in en-échelon arrays. At Locality 1 of Cerro Mocho, at Arroyo Mulichinco, they correspond to the Fracture Set 1 described by Ukar et al. (2017b). Crosscutting relationships between E-W, ENE-WSW and WNW-ESE conjugated veins and bedding reveal that most of them formed prior to folding, whereas few ones formed after bed tilting. Those fractures formed prior to folding are bed-perpendicular after restoration with respect to their adjacent bedding and were observed in all the studied areas of the Andean foothills. Contrarily, the few conjugated veins formed after bed tilting are sub-vertical and were observed in Locality 2 of Cerro Mocho and Cara Cura. In Locality 2 of Cerro Mocho, these fractures postdate basaltic dykes, form anastomosed arrays and locally show sub-horizontal strike-slip kinematic indicators such as feather fractures, as defined by Passchier and Trouw (2005). A similar situation was observed for E-W veins within the Agrio Formation and in Cara Cura, where strike-slip striae sets, and stepped slickensides have been observed. In Cerro Mocho, E-W veins postdate beef, whereas in La Yesera, Sierra de Reyes and Cara Cura this crosscutting relationship has not been identified. Veins cutting the Vaca Muerta Formation are filled with calcite cement, although ankerite cement is also observed in Cerro Mocho. In the same area, veins cutting the Tordillo Formation do not contain cement. In La Yesera, conjugated veins at the contact between the Auquilco and Tordillo Formations are filled with gypsum. In all the study areas, the orientation of E-W, ENE-WSW and WNW-ESE conjugated veins indicate E-W and ESE-WNW directions of compression.

The N–S, NNE-SSW and NNW-SSE bed-perpendicular conjugated fractures have openings of less than 2 mm and a length from 5 cm to 1 m and in most of cases they are not filled with cement. They have been observed at Cerro Mocho and Sierra de Reyes. In Locality 1 of Cerro Mocho, these fractures correspond to Fracture Sets 2, 3 and 4 described by Ukar et al. (2017b), which are postdating calcite beef and bed-perpendicular E-W veins.

7.2. Microstructural description of conjugate veins

In this section, we describe the texture of cements precipitated in E-W, ENE-WSW and WNW-ESE conjugated veins (Fig. 8). For N–S, NNE-SSW and NNW-SSE conjugated veins, this description has not been made due to the absence of cements in most of these fractures.

Cements precipitated in E-W, ENE-WSW and WNW-ESE conjugated veins display different textures and mineralogy. In Locality 1 of Cerro Mocho, E-W veins are filled with calcite and later ankerite with associated quartz (Fig. 8A). Calcite cements consist of 100–300 μm equant blocky calcite crystals, occluding completely or partially these veins. Subhedral ankerite crystals have well-defined faces and sizes from 100 to 700 μm, whereas euhedral quartz crystals have well-defined faces and are up to 1 mm long and up to 500 μm width. Occasionally, these veins are not completely occluded by cement and the remaining porosity is filled with bitumen. In Locality 2 of Cerro Mocho, up to 1 cm rhombohedral calcite crystals and accessory barite are observed in E-W veins cutting the Vaca Muerta Formation (Sample CMF31). In the same locality, calcite cement, sporadically containing solid bitumen, precipitated in anastomosed veins postdating E-W volcanic dykes with the same orientation (Fig. 8B). This cement consists of up to 3 mm equant sparite crystals and up to 1 mm long elongated sparite perpendicular and oblique to fracture walls. In these veins, multiple generations of calcite with clear crosscutting relationships are identified, indicating multiple stages of fracture opening. In Sierra de Reyes, only calcite cement has been identified within E-W, ENE-WSW and WNW-ESE conjugated veins. This cement consists of 200 μm to 2 mm crystals of equant sparite and up to 1.5 mm long elongated sparite crystals arranged perpendicular to fracture walls (Fig. 8C). In Cara Cura, 100 μm to 1 mm equant sparite crystals have been observed in E-W veins. These crystals are occasionally observed in stepped slickensides with strike-slip striae sets, which indicate the sense of shear.

8. Bed-parallel slip surfaces and faults

In addition to conjugate vein systems, bed-parallel slip surfaces, strike-slip and reverse faults have also been observed cutting beef after folding. Their crosscutting relationships are described in this section allowing the differentiation of three groups of fractures according to their relative age: 1) Beef; 2) conjugate vein systems; and 3) bed-parallel slip surfaces and strike-slip and reverse faults (Fig. 6).

8.1. Field description of bed-parallel slip surfaces and faults

Bed-parallel slip surfaces developed at the boundary between beef and the black shales of the Vaca Muerta Formation in Cerro Mocho and between carbonates and clays of the Agrio Formation in Cara Cura (Fig. 6). In Cerro Mocho, bed-parallel slip surfaces cut E-W, ENE-WSW and WNW-ESE bed-perpendicular veins and have slip indicators such as striae sets plunging in the same direction than bedding as well as steped slickensides. Contrarily, in Cara Cura these kinematic indicators and crosscutting relationships are not observed.

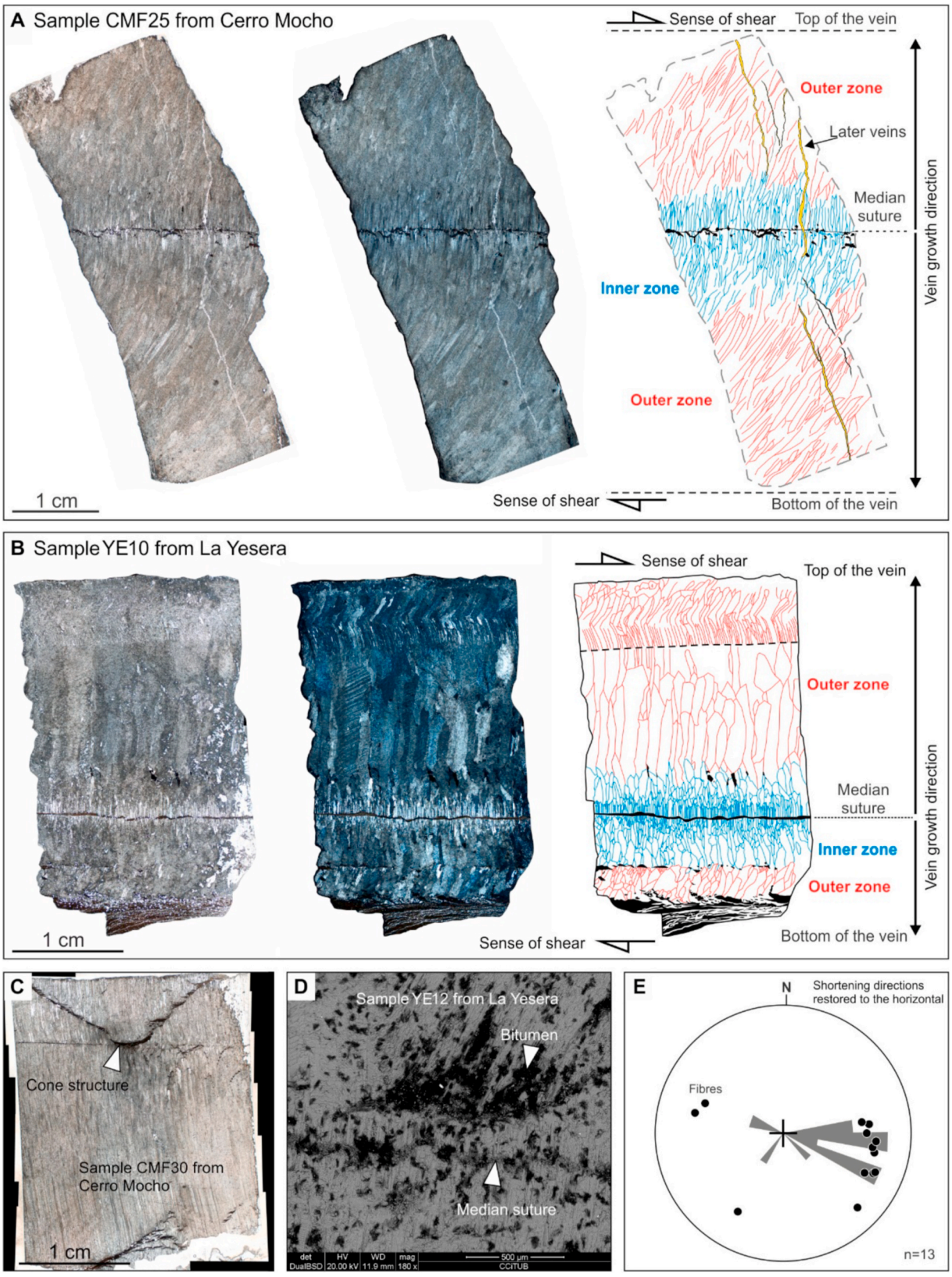

Fig. 5. Images from polarizing optical (PO) and scanning electron microscope (SEM) showing the main features of beef. A) PO images and interpretation of a beef with monoclinic symmetry. Note how elongated fibres from the outer zones indicate the sense of shear. B) PO images and interpretation of a beef with elongated fibres from outer zones perpendicular to the median suture. Repeated host rock trails (in black) indicate crack-seal mechanism for the formation of veins. C) Cone structures within the inner zone of a beef. D) Bitumen inclusions between fibres from inner zones. E) Shortening directions measured in calcite beef fibres. Orientations and dips of fibres restored to the horizontal are represented as poles. The rose diagram represents cumulative frequency of shortening orientations.

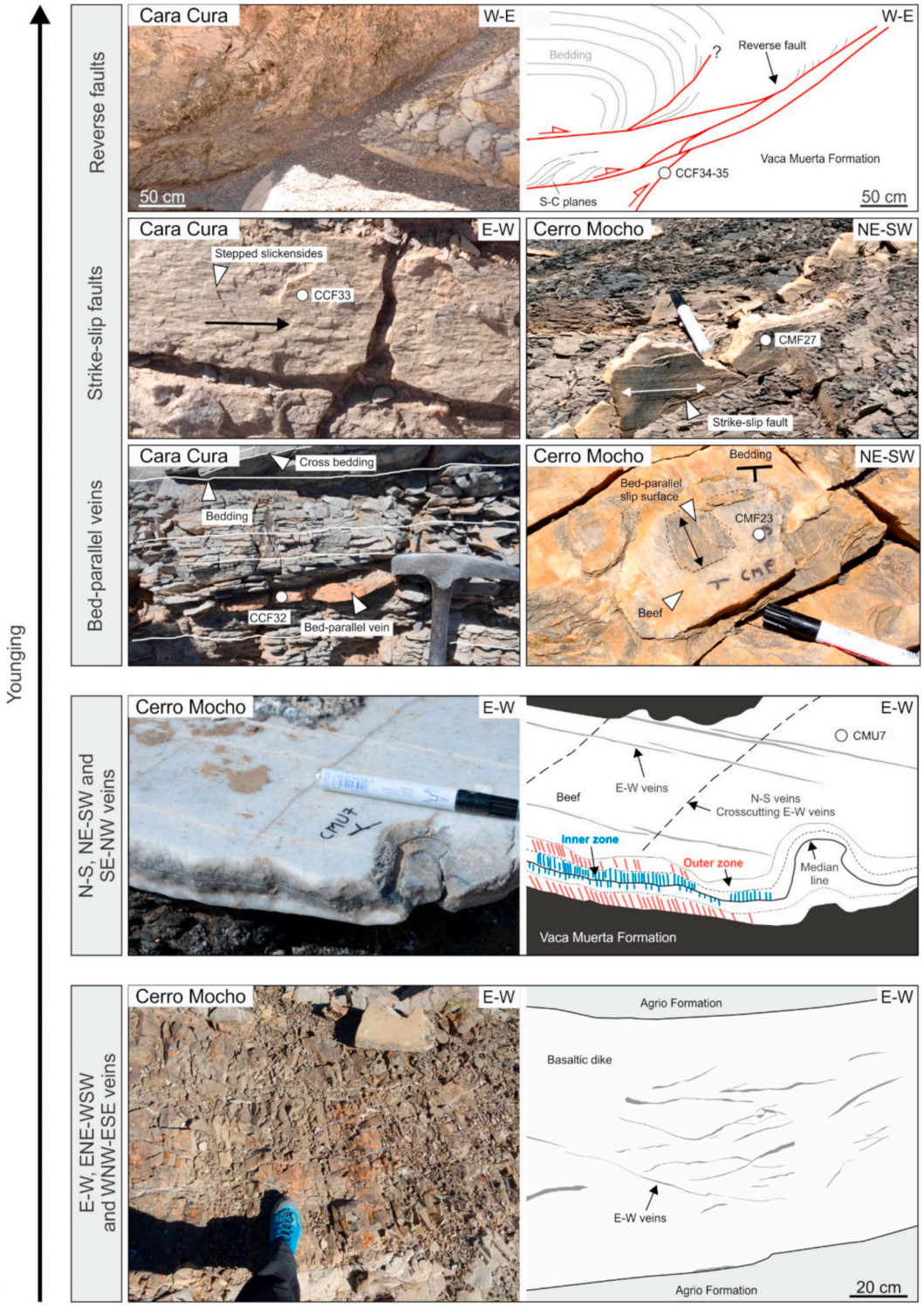

Fig. 6. Field images of the different types of fractures.

Strike-slip faults are E-W and NE-SW trending fractures that occasionally form conjugate fault systems (Figs. 6 and 7). They are scarce, consist of discrete planes dipping between 63° and 90° and have only been identified in Cerro Mocho postdating calcite beef. Strike-slip faults have a constant orientation and dip regardless bedding dips as well as subhorizontal striae sets, indicating that they formed after bed folding. In association to strike-slip faults, very local normal faults have been observed. Calcite cement only has been identified in strike-slip faults affecting the Vaca Muerta Formation, whereas cement is absent in those affecting detrital rocks of the Mulichinco Formation. Orientation of strike-slip faults in Cerro Mocho indicate ESE-WNW and NE-SW directions of compression.

Reverse faults are N–S and NW-SE trending fractures that which consist of discrete planes that dip between 6 and 41° and have been identified at Cerro Mocho and Cara Cura (Figs. 6 and 7). In Locality 1 of Cerro Mocho, and like E-W fractures, small reverse faults postdate beef and are filled with calcite and ankerite cement. Contrarily, in the Cara Cura only calcite cement has been identified. In this area, dip-slip striae

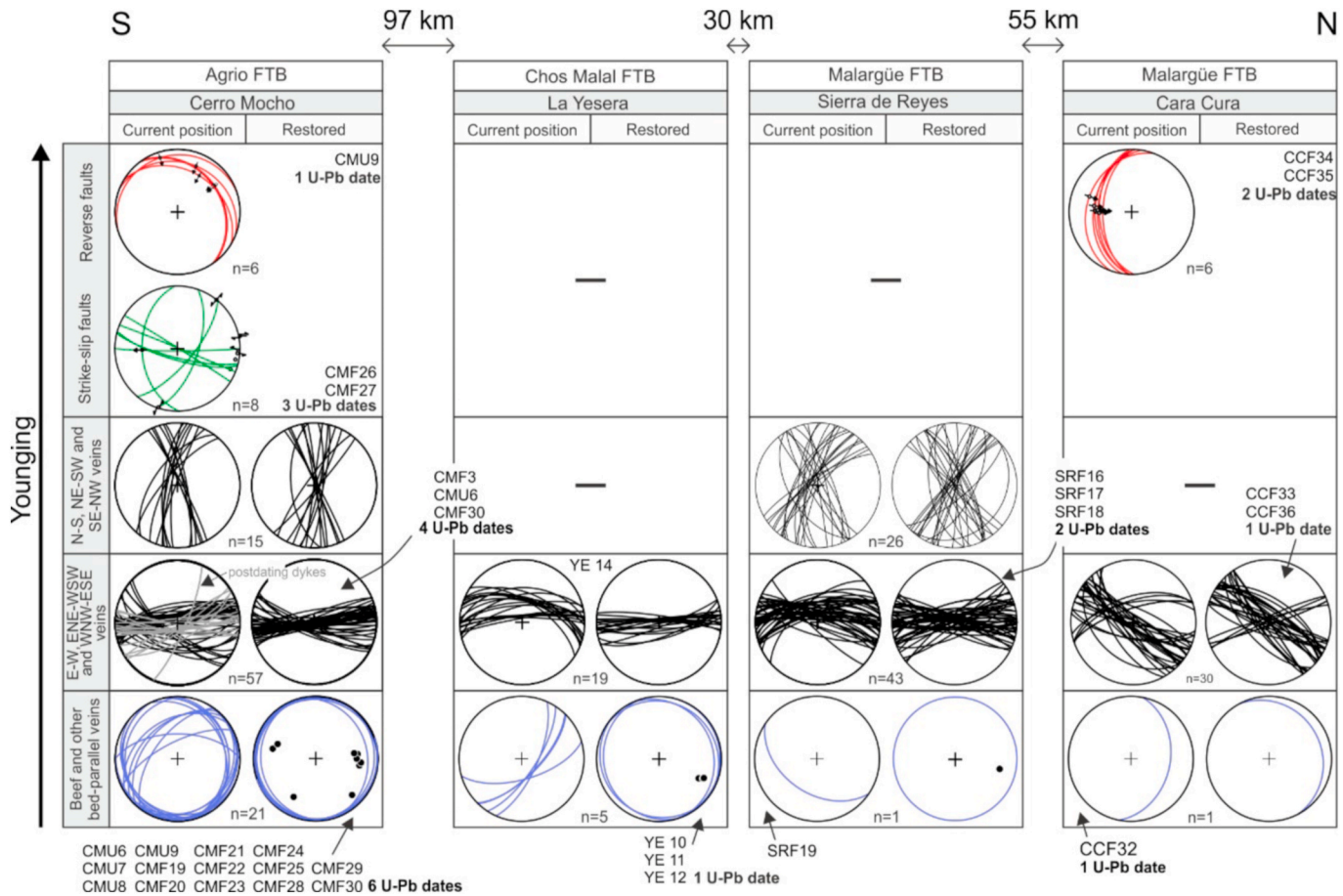

Fig. 7. Stereoplots for each type of fractures in the studied areas of the Neuquén Basin. The reference of samples and the number of measured U–Pb dates is also given. Black dots in bed-parallel veins represent orientations of fibres from beef outer zones.

sets are observed in calcite cement, and shear band cleavage developed in the host rock in association to reverse faults. Orientation of reverse faults indicate NE-SW and E-W direction of compression in Cerro Mocho and Cara Cura, respectively.

8.2. *Microstructural description of bed-parallel slip surfaces and faults*

Bed-parallel veins in Cerro Mocho postdating beef are constituted of 200 μm thick and 500 μm to 3 mm long elongated crystals parallel or oblique to fracture walls (Fig. 9A). Occasionally, 200 μm thick and up to 1 mm long elongated crystals oblique to fracture walls is also observed indicating the sense of shear during fracturing. Contrarily, calcite precipitated in bed-parallel veins from Cara Cura consist of up to 1.5 mm wide and up to 3 mm long bladed crystals.

In strike-slip faults from Locality 2 of Cerro Mocho, up to two types of cement have been identified. The first one consists of 100–300 μm thick and 1–5 mm long calcite crystals parallel to fracture walls (Fig. 9B). This calcite is dark and precipitated at the contacts with the host Vaca Muerta Formation, where strike-slip slickenlines developed. The second type of calcite cement consists of 200 μm to 1,5 mm white equant sparite (Fig. 9B). This calcite contains host rock inclusions with stylolites parallel to fracture walls at the contact with cement and precipitated in the centre of veins, between two dark calcite areas.

In reverse faults, calcite, ankerite as well as accessory quartz and barite cements have been identified. In Locality 1 of Cerro Mocho, cm scale reverse faults postdating beef contain the same equant sparite, subhedral ankerite and euhedral quartz identified in the E-W veins. In reverse faults from Cara Cura, different phases of calcite cement and accessory barite precipitated in fractures (Fig. 9C). This calcite consists of 50–700 μm equant sparite crystals precipitated in mm thick tabular bodies parallel to fracture walls and in small veinlets formed by crack seal-mechanism, which indicate the sense of shear during faulting (Fig. 9C). Barite is arranged in radial inclusions replacing calcite cement and is made of up to 200 μm long subhedral crystals.

9. U–Pb geochronology of fracture-filling carbonates

Using U–Pb dating of fracture-filling calcite and ankerite, we document 22 ages ranging from 116.7 ± 17.7 to 4.9 ± 4.9 Ma, with mean squared weighted deviation values (MSWD) lower than 2 and in general with well-defined arrays of spot analyses (Tables 1 and S2 and Figs. 10 and 11). These dates were obtained from the analysis of 53 generations of carbonate cements, indicating ~40% of dating success. In addition to these results, three additional measured dates of 69.3 ± 56.8, 2.4 ± 18.5 and −1.7 ± 43.8 have been discarded for the discussion of this study due to their high MSWD values of 5.1, 6.3 and 10.1 (samples CMU9a, CMU8C and Ye14; Table 1; Concordia Graphs in Table S2). Also, some of these discarded U–Pb ages have analytical uncertainties that are much larger than their respective U–Pb ages (CMU8C, 2.4 ± 18.5; Ye14, 3.9 ± 12.3). The same situation is observed for the sample CMU6AAa, although its MSWD is lower than 2. The analysis of this sample yielded a negative age of −1.7 ± 43.8 Ma as well as a sub-horizontal array of spot analyses, and consequently it has not considered for the discussion of the results.

Inner zones of beef within the Vaca Muerta Formation yielded six Early to Late Cretaceous dates from 116.7 ± 17.7 to 78.8 ± 10.2 Ma. Five of these dates are from Cerro Mocho and one from La Yesera (Fig. 11), whereas in Sierra de Reyes dating of beef failed. In the successful

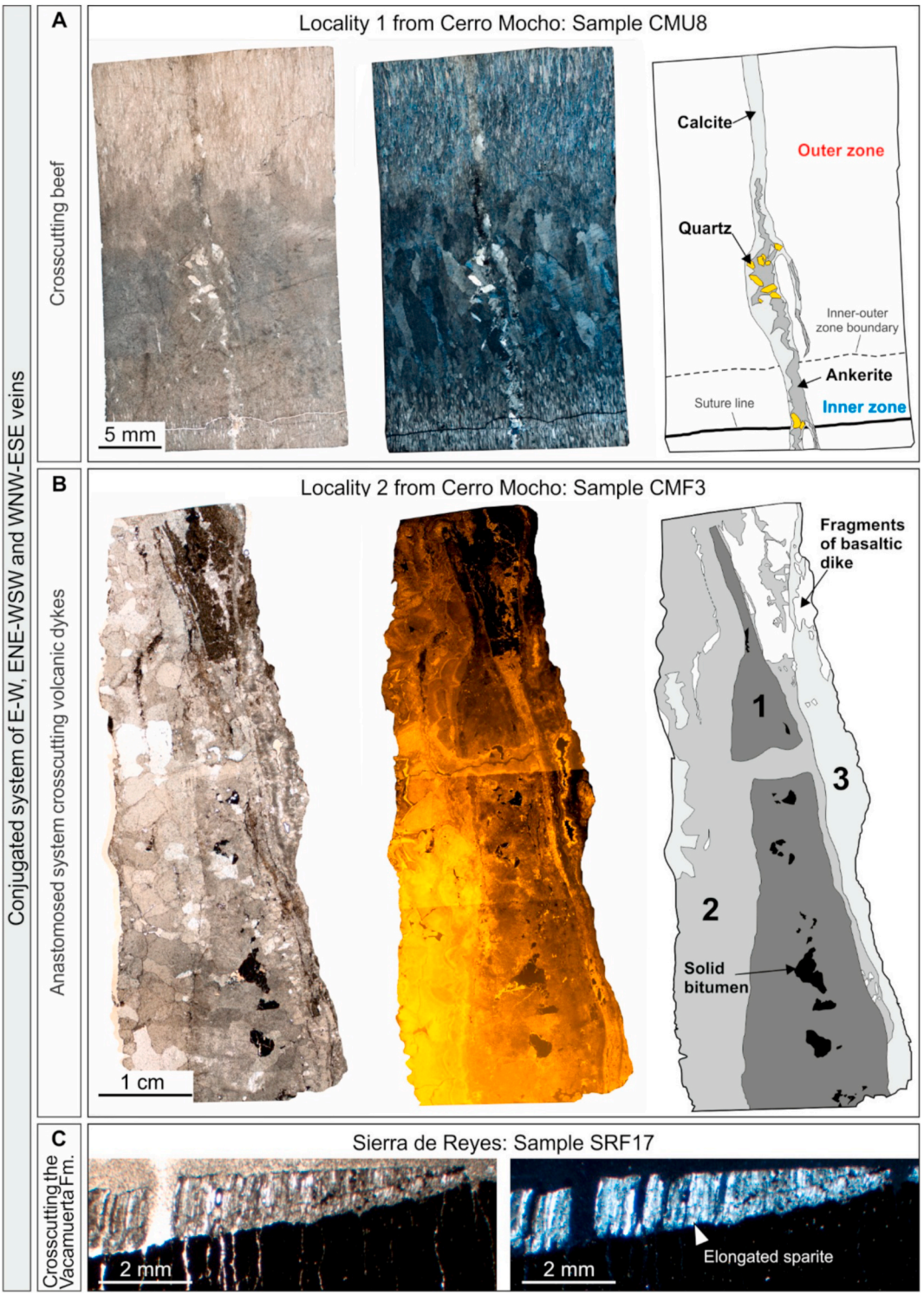

Fig. 8. Images from polarizing optical (PO) cathodoluminescence (CL) and scanning electron microscope (SEM) showing the main features of conjugated system of E-W, ENE-WSW and WNW-ESE veins. A) PO images and interpretation of an E-W vein crosscutting a beef from Locality 1 of Cerro Mocho. B) PO and Cl images and interpretation of a vein filled with three types of calcite cement (1–3) and crosscutting E-W dykes from Locality 2 of Cerro Mocho. C) PO image showing a vein from Sierra de Reyes filled with elongated crystals perpendicular to fracture walls.

samples, suitable areas for dating were only found in the vicinities of the median suture of beef. The inner zone of beef with the U–Pb age with the higher analytical error (CMF30; 87.8 ± 31.1 Ma) has a relatively high scattering of spot analyses in contrast to those beef with more accurate ages (Table S2). Despite this dispersion, spot analyses measured in sample CMF30 define a well-defined array. For outer zones only one date of 53.8 ± 48.3 Ma has been obtained in one sample from Cerro Mocho (CMU8b). The high analytical error of this sample is related to the high scatter of U–Pb data and a not well-defined array (Table S2). Therefore, the age of this sample must be considered with caution in the discussion.

For E-W, ENE-WSW and WNW-ESE conjugated veins, seven Late

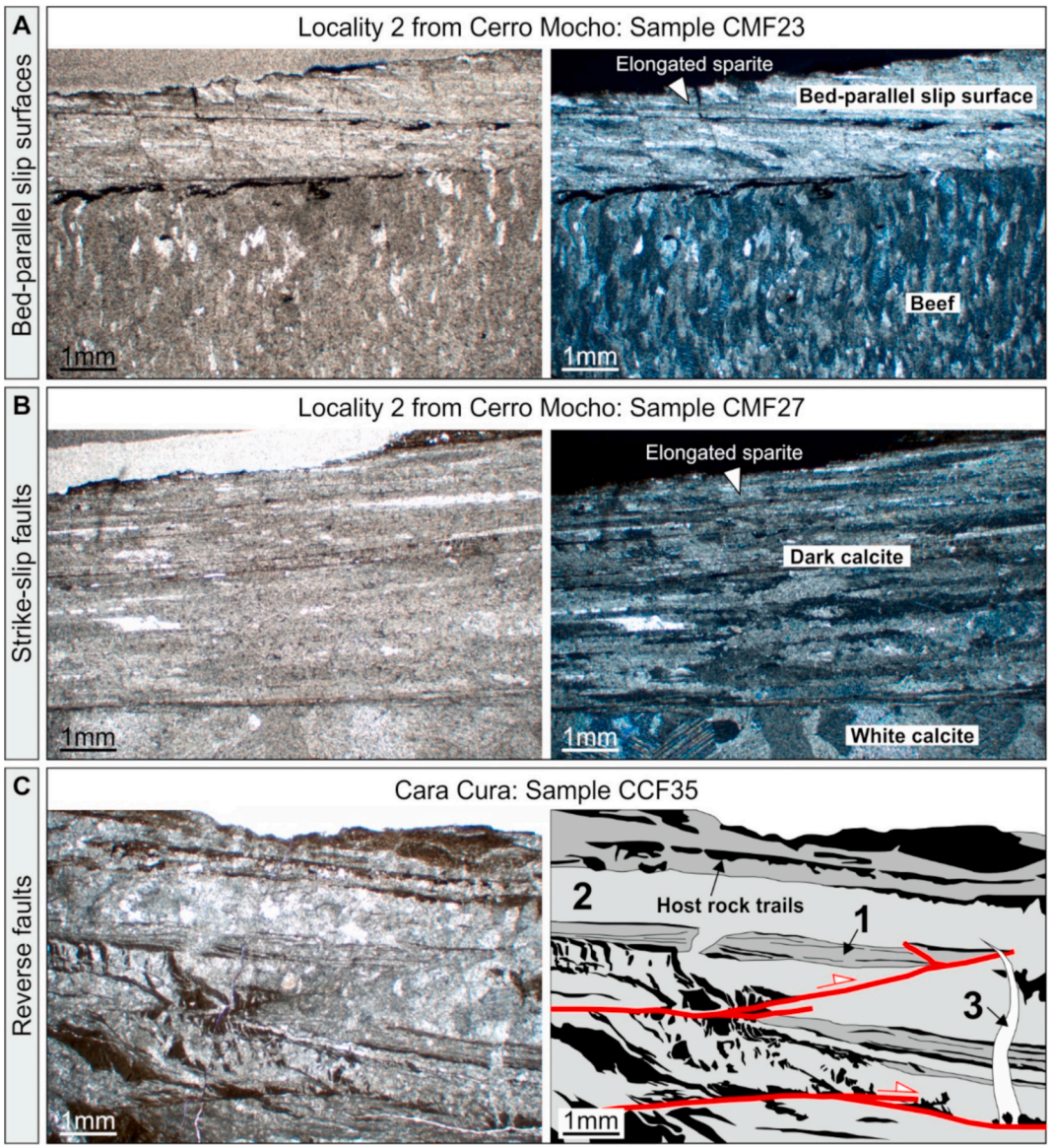

Fig. 9. Images from polarizing optical (PO) showing the main features of bed-parallel slip surfaces, strike-slip and reverse faults. A) Elongated calcite crystals parallel and oblique to fracture walls postdating a beef from Cerro Mocho. B) Elongated calcite crystals parallel to fracture walls and blocky calcite precipitated in strike-slip faults from Cerro Mocho. C) Calcite cement precipitated in a reverse fault from Cara Cura. Note how internal deformation affected different types of calcite cement (1–3).

Cretaceous to Miocene dates from 74.0 ± 12.6 to 6.2 ± 1.1 Ma have been measured (Fig. 11). Two of them were measured in ankerite cement from veins postdating beef in Locality 1 of Cerro Mocho (72.8 ± 22.4 and 60.9 ± 10.4 Ma), and five in calcite veins from Cerro Mocho at Locality 2, Sierra de Reyes and Cara Cura (74.0 ± 12.6 to 6.2 ± 1.1 Ma). Late Cretaceous dates were measured in bed-perpendicular veins, whereas the Eocene and Miocene ones have been measured in veins cutting bedding after their folding. The N–S, NE-SW and NW-SE conjugated veins were not dated by means of U–Pb dating. Despite this lack of data, crosscutting relationships with E-W, ENE-WSW and WNW-ESE bed-perpendicular veins yielding with U–Pb dates of 72.8 ± 22.4 and 60.9 ± 10.4 Ma in Locality 1 of Cerro Mocho indicate that, at least in this area, they postdate the Late Cretaceous.

One Lutetian date of 49.0 ± 3.9 Ma has been measured in calcite from one bed-parallel slip surface postdating beef in Cerro Mocho (Fig. 11). In Cara Cura, one late Miocene U–Pb age of 4.99 ± 4.95 Ma is obtained for a bed-parallel calcite vein within the Agrio Formation. Three Eocene dates from 49.9 ± 8.1 to 42.2 ± 18.9 Ma are measured in calcite precipitated in strike-slip faults cutting the Vaca Muerta Formation in Locality 2 of Cerro Mocho (Fig. 11). Finally, three dates have been measured in reverse faults (Fig. 11). In Locality 1 of Cerro Mocho, one Ypresian date of 52.0 ± 2.9 Ma is measured in ankerite cement from cm-scale reverse faults cutting beef, whereas in Cara Cura one Late Cretaceous and one Miocene date of 73.1 ± 10.7 and 9.7 ± 1.6 are obtained in a thrust affecting the Agrio Formation (CCF35b and a, respectively). However, in this sample, it is observed from crosscutting relationships that the Miocene cement (1 in Fig. 9C; CCF35a) is cut by the Late Cretaceous one (2 in Fig. 9C; CCF35b). This inconsistency could be explained by the partial replacement of the Miocene cement by barite, which could have overprinted the original U–Pb signature of calcite 1. For that reason, the Miocene U–Pb date of sample CCF35 has not been considered.

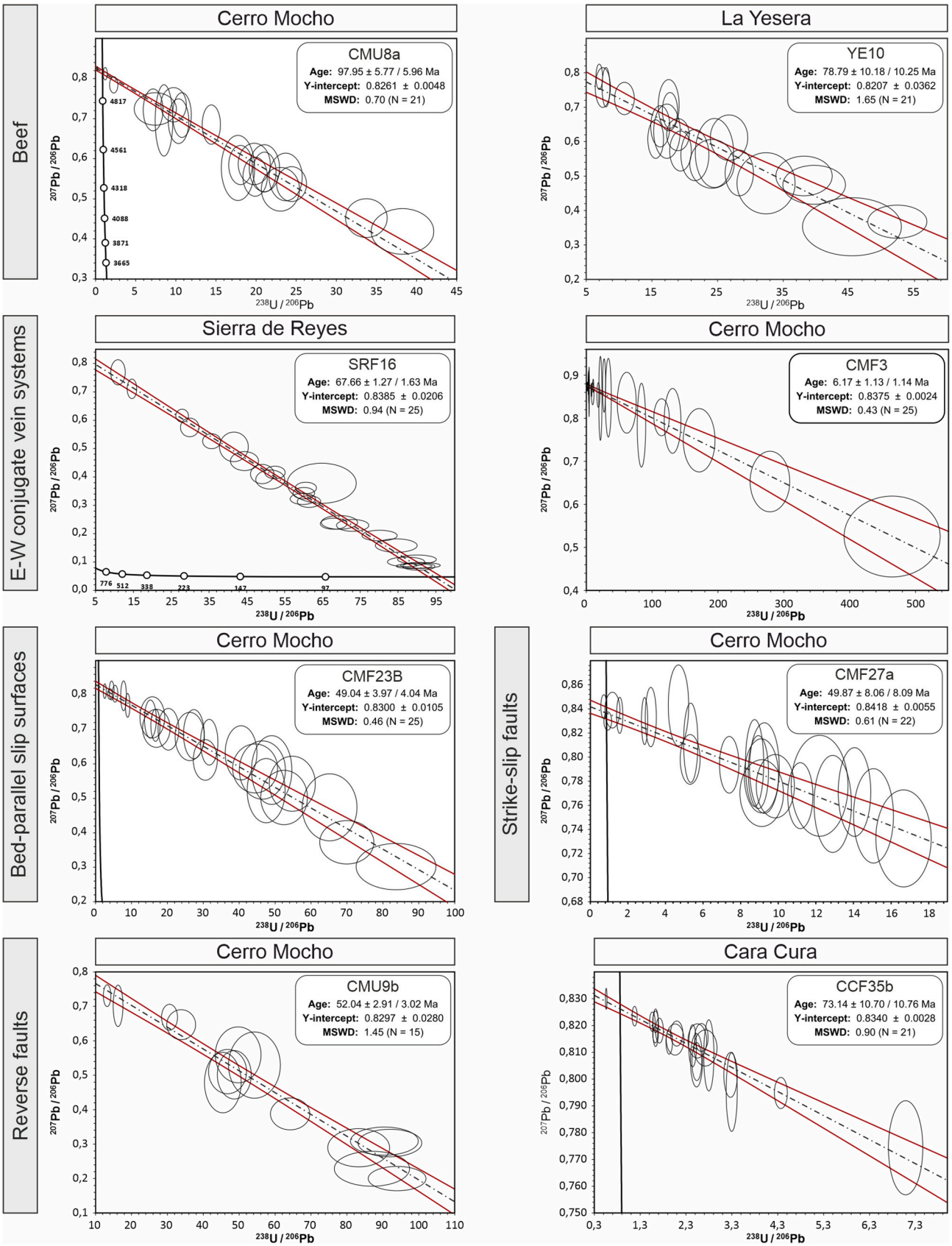

Fig. 10. Examples of Concordia graphs obtained for beef, E-W conjugate vein systems, bed-parallel slip surfaces and strike-slip and reverse faults.

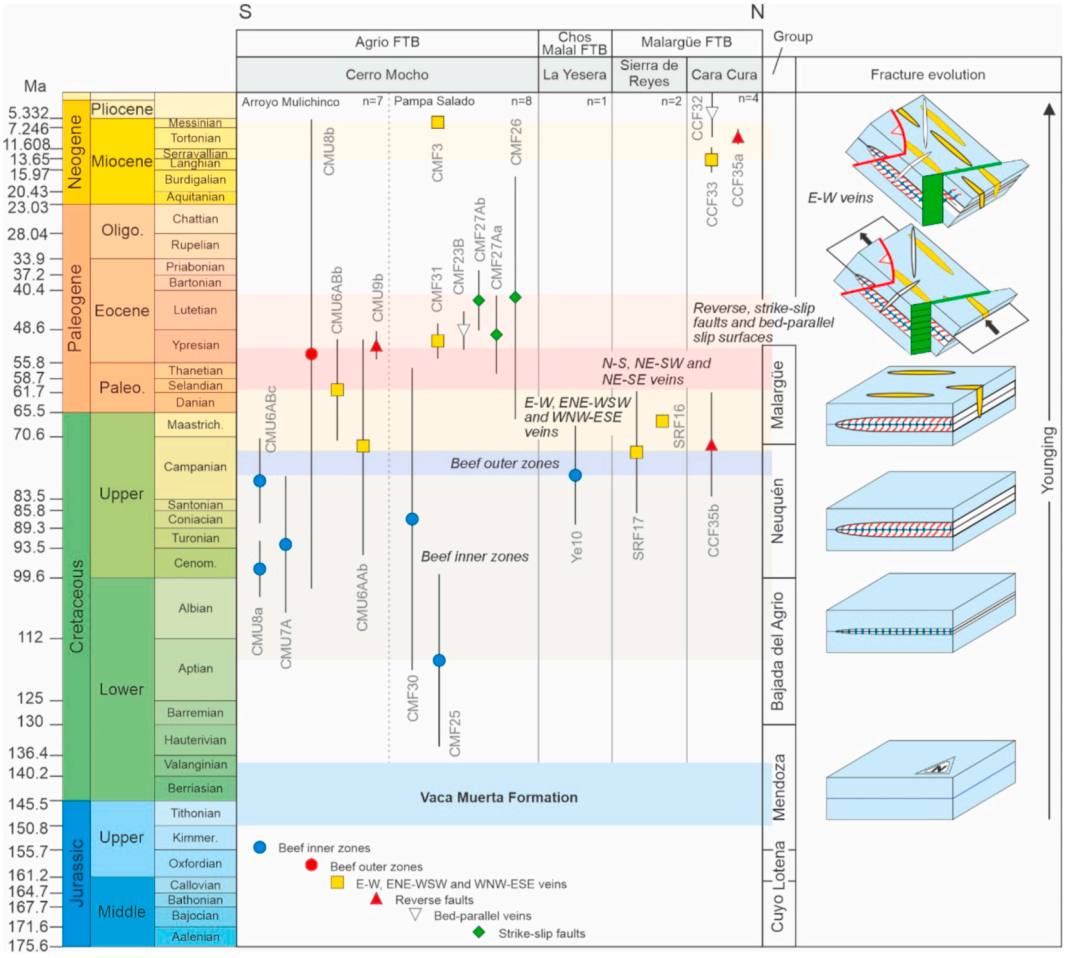

Fig. 11. Chronogram with U–Pb dates measured in the Neuquén Basin. For each result, the analytical error (black lines) and the type of fractures is also indicated. The evolution of fracturing through time is shown in the right column.

10. Discussion

10.1. Textures of fracture-filling cement: kinematic significance

The texture of the dated fracture-filling calcite and ankerite cement provides information regarding to their relationship with fracturing. Elongated sparite and fibrous textures provide evidence for syn-kinematic precipitation. These textures have been observed in calcite cement precipitated in beef, E-W, NNE-SSW and NNW-SSE conjugated veins from Sierra de Reyes and bed-parallel slip surfaces and strike-slip faults from Cerro Mocho (Fig. 8A, C and 9A, B), and thus proving that U–Pb dates in these fractures indicate the absolute timing of fracturing. Contrarily, equant sparite textures indicate crystal growth in an open space, after vein opening or at lower rates than vein opening (e.g., Beaudoin et al., 2014). However, the following microstructural features allow to interpret blocky cement as syn-kinematic as well: 1) stepped slickensides in E-W veins from Cara Cura (sample CCF33; Fig. 6); and 2) blocky crystals precipitated veins formed by crack-seal mechanism in E-W, NNE-SSW and NNW-SSE conjugated veins from Sierra de Reyes and reverse faults from Cara Cura (samples SRF16 and CCF25; Fig. 9C). These two microstructural features have not been observed in E-W, NNE-SSW and NNW-SSE conjugated veins filled with calcite and ankerite cement in Locality 1 from Cerro Mocho (sample CMU6A), although crack-seal textures along their margins have been documented for these veins by Ukar et al. (2017b). Based on the observations of the previous authors, in this study we consider that carbonate cement precipitated within conjugated veins from Cerro Mocho as syn-kinematic. For blocky calcite precipitated in bed-parallel veins in the Agrio Formation from Cara Cura (sample CCF32) and in E-W veins filled with centimetre size rhombohedral calcite crystals at Cerro Mocho (sample CMF31), syn-kinematic textures are not observed and therefore, it is not possible to confirm coeval precipitation of these cements during fracturing.

10.2. Timing of beef growth and oil generation in the andean front of Argentina

U–Pb dating of six beef inner zones yielded Aptian to Campanian ages from 116.7 ± 17.7 to 78.8 ± 10.2 Ma. The older Aptian date is within the estimated timing of formation of inner zones by Rodrigues et al. (2009) from subsidence curve analysis in the Agrio and Chos Malal fold and thrust belts. Contrarily, younger Cenomanian to Campanian dates from 97.95 ± 5.77 to 78.8 ± 10.2 Ma are within the estimated timing of formation of outer zones according to the previous authors and Ukar et al. (2020). Despite this discrepancy regarding the age of formation of inner zones, the measured U–Pb dates of beef inner zones are within the Berriasian to Maastrichtian oil window period estimated for the Vaca Muerta Formation in the Agrio, Chos Malal and Malargüe fold and thrust belts based on subsidence analysis (Cruz et al., 1996; Zapata et al., 1999; Karg and Litkke, 2020). Contrarily, although its large analytical error, the single U–Pb date of 53.8 ± 48.3 Ma measured in outer zones of beef seems to indicate that it formed during the oil-gas window transition (Fig. 12). Despite the poor quality of the U–Pb dataset obtained for beef outer zones, they probably formed soon after the growth of inner zones and before the formation of younger E-W, ENE-WSW and WNW-ESE conjugated veins with U–Pb dates from 72.8

Table 1
Summary of the U–Pb dates and MSWD values measured in fracture-filling carbonates from the Neuquén Basin. n represents the number of spots of analysis. * indicates the samples with MSWD higher than 2. Cells filled with - are from samples in which U–Pb dating failed.

Sample	Longitude	Latitude	Description	Age (Ma)	MSWD	*Upper intercepts*	*n*
Cerro Mocho Arroyo Mulichinco Locality							
CMU6AAa	38° 1′ 15.01″ S	70° 27′ 8.34″ W	E-W vein	−1.7 ± 43.8	1.88	0.7542 ± 0.0658	16
CMU6AAb	38° 1′ 15.01″ S	70° 27′ 8.34″ W	E-W vein	72.8 ± 22.4	1.19	0.8598 ± 0.0165	15
CMU6ABb	38° 1′ 15.01″ S	70° 27′ 8.34″ W	E-W vein	60.9 ± 10.4	0.26	0.8673 ± 0.0181	18
CMU6ABc	38° 1′ 15.01″ S	70° 27′ 8.34″ W	Beef inner zone	79.63 ± 8.69	0.58	0.8660 ± 0.0193	21
CMU7A	38° 1′ 15.10″ S	70° 27′ 8.19″ W	Beef inner zone	92.92 ± 14.03	0.98	0.8330 ± 0.0107	25
CMU8a	38° 1′ 14.94″ S	70° 27′ 7.88″ W	Beef inner zone	97.95 ± 5.77	0.70	0.8261 ± 0.0048	21
CMU8b	38° 1′ 14.94″ S	70° 27′ 7.88″ W	Beef outer zone	53.8 ± 48.3	1.32	0.7324 ± 0.0772	21
CMU8C*	38° 1′ 14.94″ S	70° 27′ 7.88″ W	E-W vein	2.4 ± 18.5	6.30	0.7400 ± 0.0671	21
CMU9a*	38° 1′ 16.13″ S	70° 27′ 6.38″ W	Beef inner zone	69.3 ± 56.8	5.06	0.7630 ± 0.1196	20
CMU9b	38° 1′ 16.13″ S	70° 27′ 6.38″ W	Small reverse fault	52.0 ± 2.9	1.45	0.8297 ± 0.0280	15
Cerro Mocho Pampa Salado Locality							
CMF2	38° 8′ 33.14″ S	70° 9′ 6.06″ W	E-W vein	–	–	–	–
CMF3	38° 8′ 33.27″ S	70° 9′ 6.21″ W	E-W vein	6.2 ± 1.1	0.43	0.8375 ± 0.0024	25
CMF19	38° 8′ 16.31″ S	70° 26′ 24.01″ W	Beef	–	–	–	–
CMF20	38° 8′ 16.81″ S	70° 26′ 24.40″ W	Beef	–	–	–	–
CMF23B	38° 7′ 37.67″ S	70° 26′ 10.02″ W	Bed-parallel slip surface	49.0 ± 3.9	0.46	0.8300 ± 0.0105	25
CMF24	38° 7′ 37.61″ S	70° 26′ 10.12″ W	Beef	–	–	–	–
CMF25a	38° 7′ 17.67″ S	70° 25′ 48.17″ W	Beef inner zone	116.7 ± 17.7	1.29	0.8466 ± 0.0069	24
CMF26	38° 7′ 17.63″ S	70° 25′ 48.17″ W	Normal fault?	42.2 ± 18.9	0.90	0.8290 ± 0.0082	18
CMF27a	38° 7′ 17.48″ S	70° 25′ 48.22″ W	Strike-slip fault	49.9 ± 8.1	0.61	0.8418 ± 0.0055	22
CMF27b	38° 7′ 17.48″ S	70° 25′ 48.22″ W	Strike-slip fault	42.8 ± 6.2	0.67	0.8370 ± 0.0101	20
CMF28	38° 7′ 4.48″ S	70° 24′ 25.06″ W	Beef	–	–	–	–
CMF30	38° 7′ 4.32″ S	70° 24′ 24.88″ W	Beef inner zone	87.8 ± 31.1	1.14	0.8433 ± 0.0177	24
CMF31	38° 7 ‘4.54″ S	70° 24′ 25.01″ W	E-W vein	51.2 ± 3.6	0.79	0.8633 ± 0.0143	23
La Yesera							
Ye10	37° 17′ 19.28″ S	69° 51′ 41.79″ W	Beef inner zone	78.8 ± 10.2	1.65	0.8207 ± 0.0362	21
Ye11	37° 17′ 19.46″ S	69° 51′ 41.07″ W	Beef	–	–	–	–
Ye12	37° 17′ 19.24″ S	69° 51′ 41.43″ W	Beef	–	–	–	–
Ye14*	37° 17′ 19.42″ S	69° 51′ 42.10″ W	E-W vein	3.9 ± 12.3	10.13	0.7191 ± 0.0386	23
Sierra de Reyes							
SRF16	37° 1′ 54.87″ S	69° 42′ 32.95″ W	E-W vein	67.7 ± 1.3	0.94	0.8385 ± 0.0206	25
SRF17	37° 1′ 50.80″ S	69° 42′ 21.13″ W	E-W vein	74.0 ± 12.6	0.60	0.8350 ± 0.0039	15
SRF19	37° 2′ 9.28″ S	69° 42′ 29.42″ W	Beef	–	–	–	–
Cara Cura							
CCF32	36° 33′ 27.25″ S	69° 32′ 44.64″ W	Bed-parallel vein	4.9 ± 4.9	0.44	0.8103 ± 0.0054	23
CCF33	36° 33′ 24.40″ S	69° 32′ 40.80″ W	E-W vein	13.9 ± 2.6	0.73	0.8218 ± 0.0037	22
CCF35a	36° 33′ 31.53″ S	69° 32′ 30.97″ W	Reverse fault	9.7 ± 1.6	0.64	0.7875 ± 0.0108	21
CCF35b	36° 33′ 31.53″ S	69° 32′ 30.97″ W	Reverse fault	73.1 ± 10.7	0.90	0.8340 ± 0.0028	21
CCF36	36° 33′ 29.73″ S	69° 32′ 32.80″ W	E-W vein	–	–	–	–

± 22.4 to 60.9 ± 10.4 Ma.

Subsidence curve analysis was carried out by Zapata et al. (1999) in the footwall of the Agrio fold and thrust belt at Nanauco-Loma Rayoso section of Rojas Vera et al. (2015) and at Arroyo Mulichinco outcrop by Ukar et al. (2020). If we take these curves as representative for Cerro Mocho area, and we project the U–Pb dates of beef inner zones on it, we observe that they formed during burial of the Neuquén basin within the oil window (Fig. 12). Likewise, the U–Pb dates measured in beef inner zones from La Yesera, in the hangingwall of the Chos Malal fold and thrust belt, also precipitated in the oil window (Fig. 12).

After unfolding beef together with bedding to the horizontal, the restored disposition of fibres from outer zones of the studied beef evidence that they formed in a period of layer-parallel shortening. Contrarily, the disposition of sub-vertical fibres in the inner zones with measured U–Pb dates from 116.7 ± 17.7 to 78.8 ± 10.2 Ma does not show evidence of sub-horizontal deformation. The older age of the beef with a U–Pb age of 116.7 ± 17.7 Ma and the errors of beef with ages of 92.92 ± 14.03, 97.95 ± 5.77 and 87.8 ± 31.1 Ma indicate that these inner zones could have formed prior to the beginning of the Andean compression, which is dated at around 100 Ma according to Zamora-Valcarce et al. (2006) and Tunik et al. (2010). Contrarily, most of the U–Pb ages and their analytical errors measured in beef inner zones fall within the timing of deposition of the Neuquén Group, which registers the initial stages of foreland conditions and compression in the Neuquén Basin (Tunik et al., 2010). The interplay between tectonic stresses and burial of the Vaca Muerta Formation triggering beef growth is reconstructed during the deposition of the Neuquén group in Fig. 13. According to Cobbold and Rodrigues (2007), if rocks fail in shear, newly formed bed-parallel fractures will be conical and dilatant, leading to the development of cone-in-cone structures. These observations agree with the work of Zanella et al. (2021) comparing calcite beefs from different foreland basins worldwide and U–Pb dating of one beef within the Paris basin coevally with compressional deformation. These authors concluded that growth of bed-parallel beef in foreland settings may be enhanced by external tectonic stresses in addition to overpressures caused by organic matter maturation related to burial. This scenario fits with the U–Pb results presented in this study and the occurrence of cone-in-cone structures in beef inner zones from the Neuquén Basin.

Beef within the Vaca Muerta Formation have suffered different burial conditions at Cerro Mocho, La Yesera and Sierra de Reyes (Fig. 12). These differences could have resulted in different timings of oil maturation and growth of beef inner zones. In the study area, the youngest age of beefs has been measured at La Yesera (78.8 ± 10.2 Ma), where the Vaca Muerta Formation has a thickness of 412 m. Contrarily, at Cerro Mocho, beef inner zones yielded older ages between 116.7 ± 17.7 and 79.63 ± 8.69 Ma (Fig. 11). However, the absence of a large U–Pb dataset in the La Yesera and in Sierra de Reyes does not allow to reveal a younging trend from deeply buried domains of the Neuquén Basin (Cerro Mocho) to shallower positions (La Yesera and Sierra de Reyes).

10.3. Fracture evolution linked to andean shortening

The U–Pb dating of fracture-filling calcite and ankerite cement from in the Neuquén Basin together with the structural analysis of fractures

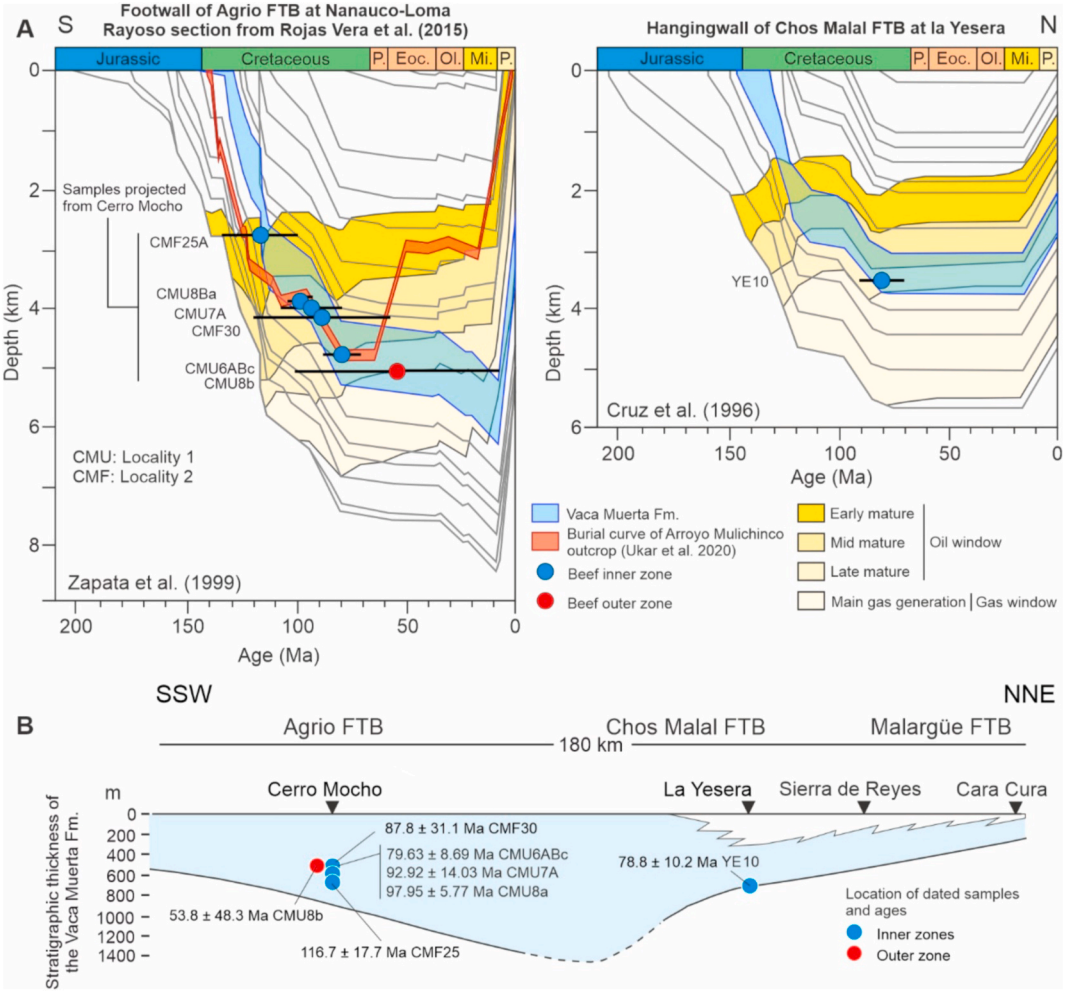

Fig. 12. A) Calculated burial curves and organic matter maturity for the footwall of Chos Malal and hangingwall of Agrio fold and thrust belts based on Cruz et al. (1996) and Zapata et al. (1999), respectively. The calculated burial curve for the Arroyo Mulichinco outcrop of Ukar et al. (2020) is also included. La Yesera and Cerro Mocho are in the Chos Malal and Agrio fold and thrust belts, respectively. The burial curves also include the U–Pb dates measured in beef. Samples in the footwall of the Agrio fold and thrust belt are projected from Cerro Mocho. The position of beef with respect to the bottom of the Vaca Muerta Formation is based on B. B) Geological cross-section of the Vaca Muerta Formation along the studied area indicating the position of dated calcite beef and their age in millions of years (Ma).

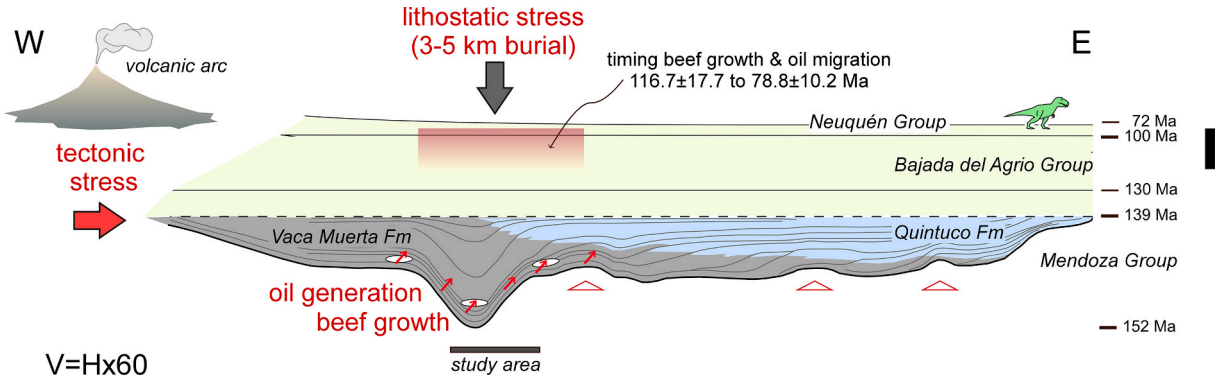

Fig. 13. W-E regional sketch of the Neuquén Basin where is shown the interplay between burial of the Vaca Muerta formation and tectonic stresses triggering beef growth and oil generation. The Vaca Muerta and Quintuco distribution is based on Dominguez et al. (2020).

reveal 3 compressive periods: Early Cretaceous-late Palaeocene, late Palaeocene-late Eocene and middle-late Miocene (Fig. 14). For the first time, beef and other fractures linked to the growth of the Andean front in the Agrio, Chos Malal and Malargüe fold and thrust belts have been dated.

Early Cretaceous-late Palaeocene compression is identified in beef and E-W, ENE-WSW and WNW-ESE bed-perpendicular veins with U–Pb dates from 116.7 ± 17.7 to 60.9 ± 10.4 Ma (Fig. 14). Beef inner zones register mild compression pulses unable to generate microstructures such as oblique fibres related to tectonic deformation between 100 and 78.8 ± 10.2 Ma. Contrarily, the orientation of calcite crystals in younger beef outer zones and in bed-perpendicular veins after their restoration

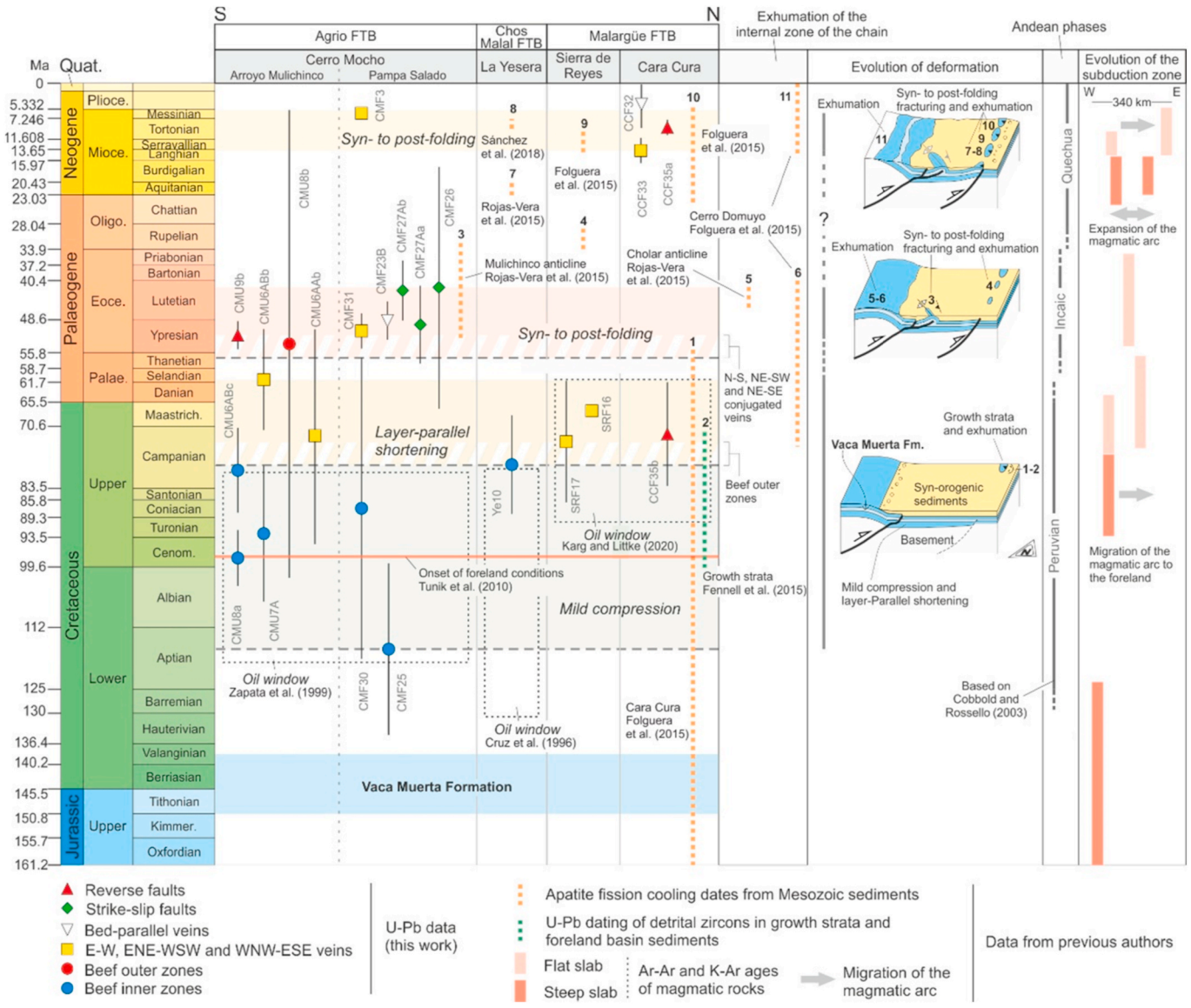

Fig. 14. Evolution of the studied sector of the Neuquén Basin from Early Cretaceous to Miocene. Apatite fission tracks data are from Folguera et al. (2015 and Rojas Vera et al. (2015). U–Pb dates of detrital zircons in growth strata and foreland sediments are from Tunik et al. (2010) and Fennell et al. (2015). Frames indicating the timing of the oil window are based on Cruz et al. (1996), Zapata et al. (1999) and Karg and Litkke (2020). The tectonic phases of the Andes are based on Cobbold and Rossello (2003). Ages and position of igneous rocks are based on Munigaza et al., 1985, Llambías and Rapela (1989); Mpodozis and Ramos (1989); Ramos and Barbieri (1989); Jordan et al. (2001); Radic et al. (2002); Franchini et al. (2003); Ramos et al. (2014); Iannelli et al. (2017); Gianni et al. (2017), 2018; Fennell et al. (2019). The evoltion of the subduction zone is based on Ramos and Folguera (2005).

with respect to bedding indicate that they formed during E-W layer-parallel shortening, which probably began after 78.8 ± 10.2 Ma, after the growth of beef inner zones and oil generation. The oldest U–Pb age of 116.7 ± 17.7 Ma measured in beef inner zones roughly coincides with the age of onset of the Andean compression and of the Andean foreland as proposed by Zamora Valcarce et al. (2006) and Tunik et al. (2010), respectively (Fig. 14). This first compressional event, identified in the frontal areas of the Andean system, is also proven during the Late Cretaceous in the innermost parts of Agrio, Chos Malal and Malargüe fold and thrust belts. Apatite Fission Track (AFT) ages from western Cordillera del Viento and Cholar anticline indicate late Cretaceous-Palaeocene exhumation linked to the inversion tectonics of normal faulted blocks (Folguera et al., 2015; Rojas Vera et al., 2015) (Fig. 14). Late Cretaceous exhumation based on AFT ages is also documented in the Cara Cura frontal anticline (Rojas Vera et al., 2015), coinciding with one of our Campanian ages at 73.1 ± 10.7 Ma obtained in a reverse fault in the same locality (Fig. 14). This older group of ages, indicating compression during the early Cretaceous-late Palaeocene, is consistent with the Peruvian tectonic phase defined by Steinmann (1929). An E-W shortening direction is obtained from our structural analysis of sampled fractures with Early Cretaceous–Palaeocene ages, consistent with orthogonal plate convergence described by Pardo-Casas and Molnar (1987) for this period. The measured E-W shortening direction also coincides with the observations of Cobbold and Rosello (2003), which indicate an E-W direction of compression based on the N–S direction of the Agua Amarga thrust that was active from Aptian to Campanian.

Late Cretaceous to Palaeocene layer-parallel shortening was followed by the development of N–S, NE-SW and NW-SE bed-perpendicular conjugated veins at Cerro Mocho. Crosscutting relationships with older beef outer zones and E-W, ENE-SSW and WNW-SSE conjugated veins yielding U–Pb dates from 78.8 ± 10.2 Ma to 60.9 ± 10.4 Ma indicate that they formed during the late Palaeocene (Fig. 14). After this period, Eocene compression is identified at Cerro Mocho in calcite cement filling

strike-slip and reverse faults and bed-parallel slip surfaces with U–Pb dates from 52.0 ± 2.9 to 42.2 ± 18.9 Ma, although analytical errors of these dates suggest that this deformation period could have developed from latest Palaeocene to latest Eocene (and probably to the Early Oligocene; Fig. 14). Structural analysis of fractures indicates syn-to post-folding deformation after the formation of N–S, NE-SW and NW-SE bed-perpendicular conjugated veins because: 1) strike-slip and reverse faults cut already folded beds; and 2) bed-parallel slip surfaces are interpreted in other orogens worldwide as the result of flexural slip (Jessel et al., 1994; Travé, 1997; Tavani et al., 2015). This period of syn-to post folding deformation matches with the exhumation of the Agrio and Malargüe fold and thrust belts since the early Eocene according to AFT ages from 52.9 to 30 Ma measured in the Mulichinco anticline and Sierra de Reyes (Folguera et al., 2015; Rojas Vera et al., 2015, Fig. 14). Furthermore, the late Palaeocene-Eocene compressional period identified from U–Pb dating also agrees with development of an angular unconformity between the latest Cretaceous-earliest Eocene Malargüe Group and the late Oligocene Palaoco Formation in the eastern flank of the frontal Sierra de Reyes anticline (Cobbold and Rossello, 2003; Rojas Vera et al., 2014; Sagripanti et al., 2012). This indicates that the late Palaeocene-late Eocene U–Pb dates measured in reverse and strike-slip faults from Cerro Mocho constrain the timing of growth of the Arroyo Mulichinco anticline and the orogenic front. This orogenic growth was also documented by Ukar et al. (2020) from subsidence curve analysis. These authors estimated the uplift of the Agrio fold and thrust belt, in the study area and to the east of the Andean front since the Palaeocene and Miocene, respectively. Ukar et al. (2020) also estimated Late Cretaceous to Palaeocene ages for beef growth in Arroyo Mulichinco, whereas to the east of the Andean front, Late Cretaceous to Miocene ages were estimated. This discrepancy of beef growth ages could be related to the older uplift of the Agrio fold and thrust belt during the Paleogene, a period that coincide with the U–Pb ages measured in reverse and strike slip faults and bed-parallel slip surfaces from Cerro Mocho. The NE-SW orientation of compression measured in these faults is consistent with the Incaic phase of the Andes, which has been identified in NE-SW bitumen dykes, synclines near Collipilli and the Cortaderas thrust by Cobbold and Rossello (2003). Such oblique convergence is the result of the NE-directed motion of the Farallon plate that took place during the same period according to Pardo-Casas and Molnar (1987), Scheuber et al. (1994) and Somoza and Ghidella (2012).

Miocene compression is recognized in E-W veins with U–Pb dates from 13.9 ± 2.6 to 6.2 ± 1.1 Ma cutting folded volcanic dykes at Cerro Mocho and folded Agrio Formation at Cara Cura (Fig. 14). This period of deformation coincides with AFT data from La Yesera, Sierra de Reyes and Cara Cura revealing an exhumation event that began during the late Oligocene at 25 Ma and continued during the late Miocene at 5 Ma and to the present day (Guzmán et al., 2007; Colavitto et al., 2009; Messager et al., 2010; Folguera et al., 2015; Sánchez et al., 2018). This exhumation resulted in the unroofing of the Agrio, Chos Malal and Malargüe fold and thrust belts due to the uplift of frontal structures and the deposition of growth strata during the Miocene (Sagripanti et al., 2012, 2016, 2016; Horton et al., 2016). The E-W orientation of compression inferred for veins with Miocene U–Pb dates is consistent with more orthogonal plate convergence during the Miocene according to Pardo-Casas and Molnar (1987), Scheuber et al. (1994) and Somoza and Ghidella (2012). This orientation is also in accordance with the Quechua phase of the Andes, also identified in other Neogene structures of the Neuquén Basin such as the Huantraico syncline and the Tromen thrusts (Cobbold and Rossello, 2003; Galland et al., 2007).

Finally, U–Pb dates presented in this study show a relationship with the subduction history of the Nazca-Farallon plate. In this line, the late Palaeocene-Eocene and middle-late Miocene periods of syn-to post-folding deformation identified in the Andean foothills from U–Pb dating coincide with periods of flat subduction of the Pacific slab beneath the Andes and variable convergence angles, which are accompanied with the forelandward migration of the related magmatic arc (e.g., Pardo-Casas and Molnar, 1987; Ramos and Folguera, 2005; Rodrigues et al., 2009; Sagripanti et al., 2016; Gianni et al., 2017; Horton, 2018; Chen et al., 2019, Fig. 14).

11. Conclusions

The structural analysis of fractures combined with petrographic observations and 22 U–Pb dates measured in calcite and ankerite cement precipitated in bed-parallel calcite beef as well as bed-perpendicular veins and faults at the front of Agrio, Chos Malal and Malargüe fold and thrust belts constrained the absolute ages of beef growth and three Andean shortening periods.

The close relationship between beef growth and oil generation is registered in inner zones of beef from Cerro Mocho and La Yesera, yielding U–Pb dates from 116.7 ± 17.7 to 78.8 ± 10.2 Ma (Aptian to Campanian). The inner zones of beef formed during burial of the Vaca Muerta Formation within the oil window, determined by integrating U–Pb dates with published burial curves.

U–Pb dating of beef inner zones reveals that some of these formed prior to the Andean compression, whereas most of them formed coevally with the deposition of the Neuquén Group. These results, together with the occurrence of cone-in-cone structures, confirm that tectonic pulses related to the Andean compression may enhance beef growth, as has been observed previously in other fold and thrust belts worldwide. Crosscutting relationships between beef inner zones and younger E-W, ENE-WSW and WNW-ESE bed-perpendicular conjugated veins with U–Pb dates from 72.8 ± 22.4 to 60.9 ± 10.4 Ma constrain the youngest ages of growth of outer zones of beef.

A first and long early Cretaceous to late Palaeocene compressional period is identified in both calcite beef and E-W, ENE-WSW and WNW-ESE bed-perpendicular conjugated fractures filled with calcite and ankerite cement. Beef inner zones register mild tectonic pulses from 116.7 ± 17.7 to 78.8 ± 10.2 Ma, whereas beef outer zones and bed-perpendicular veins register a period of east-directed layer-parallel shortening from 78.8 ± 10.2 to 60.9 ± 10.4 Ma. These results, based on 10 U–Pb dates from Cerro Mocho, La Yesera and Sierra de Reyes, indicate that layer-parallel shortening ended in these localities around to the Palaeocene-Eocene boundary.

Two periods of syn-to post-folding fracturing during the lower-middle Eocene and middle-late Miocene followed layer-parallel shortening in the study region. The lower-middle Eocene one is identified in calcite cement filling strike-slip and reverse faults and bed-parallel slip surfaces from Cerro Mocho with ages from 52.0 ± 2.9 to 42.2 ± 18.9 Ma (n = 6). This minimum Eocene duration of NE-SW local compression fits with published AFTA results constraining the growth of the Arroyo Mulichinco anticline and the Andean front. The middle-late Miocene second period of syn-to post-folding fracturing is dated in E-W calcite veins from Cerro Mocho and Cara Cura with ages from 13.9 ± 2.6 to 6.2 ± 1.1 Ma (n = 3). The minimum duration of this second event matches with published AFT data documenting the structural growth and exhumation of Cara Cura and Sierra de Reyes anticlines.

The lower-middle Eocene and middle-late Miocene periods of syn-to post-folding fracturing identified from our new U–Pb ages occurred coevally to periods of flat subduction of the Nazca-Farallon plate beneath the Andes.

Declaration of competing interest

The authors declare that they have no known competing financial interests or personal relationships that could have appeared to influence the work reported in this paper.

Acknowledgements

This research is a contribution of the Group of Dynamics of the Lithosphere (GDL), Geosciences Barcelona (Geo3Bcn), Consejo Superior

de Investigaciones Científicas (CSIC), Spain. This work was partially funded by Equinor Research Center, Bergen (Norway) and Subtetis project (PIE–CSIC–201830E039). This research is within the framework of the Grups Consolidats de Recerca "Modelització Geodinàmica de la Litosfera" (2017SGR-847) and "Geologia Sedimentària" (2017SGR-824). U–Pb geochronology was accomplished at FIERCE (Frankfurt Isotope and Element Research Center, Goethe University). This is FIERCE contribution No. 73. We thank the accurate and constructive reviews from Alain Zanella, an anonymous reviewer and the editor Nicolas Beaudoin, which greatly improved this manuscript.

Appendix A. Supplementary data

Supplementary data to this article can be found online at https://doi.org/10.1016/j.marpetgeo.2021.105204.

References

Aguirre-Urreta, B., Tunik, M., Naipauer, M., Pazos, P., Ottone, E., Fanning, M., Ramos, V. A., 2011. Malargüe group (Maastrichtian–Danian) deposits in the Neuquén Andes, Argentina: implications for the onset of the first atlantic transgression related to western Gondwana break-up. Gondwana Res. 19, 482–494.

Aguirre-Urreta, B., Schmitz, M., Lescano, M., Tunik, M., Rawson, P.F., Concheyro, A., Buhler, M., Ramos, V.A., 2017. A high precision U–Pb radioisotopic age for the Agrio Formation, Neuquén basin, Argentina: implications for the chronology of the hauterivian stage. Cretac. Res. 75, 193–204.

Aguirre-Urreta, B., Naipauer, M., Lescano, M., López-Martínez, R., Pujana, I., Vennari, V., Lena, L.F.D., Concheyro, A., Ramos, V.A., 2019. The Tithonian chrono-biostratigraphy of the Neuquén Basin and related Andean areas: a review and update. J. S. Am. Earth Sci. 92, 350–367.

Arregui, C., Carbone, O., Martínez, R., 2011a. El Grupo Cuyo (Jurásico Temprano-Medio) en la Cuenca Neuquina. In: Leanza, H., Arregui, C., Carbone, O., Danieli, J.C., Vallés, J.M. (Eds.), Relatorio del XVIII COngreso Geológico Argentino. Asociación Geológica Argentina, Neuquén, pp. 77–89.

Arregui, C., Carbone, O., Sattler, F., 2011b. El Grupo Lotena (Jurásico Medio-Tardío) en la Cuenca Neuquina. In: Leanza, H., Arregui, C., Carbone, O., Danieli, J.C., Vallés, J. M. (Eds.), Relatorio del XVIII COngreso Geológico Argentino. Asociación Geológica Argentina, Neuquén, pp. 91–98.

Barrio, C.A., 1990. Late Cretaceous Early Tertiary sedimentation in a semi-arid foreland basin (Neuquén basin, western Argentina). Sediment. Geol. 66, 255–275.

Beaudoin, N., Bellahsen, N., Lacombe, O., Emmanuel, L., Pironon, J., 2014. Crustal-scale fluid flow during the tectonic evolution of the Bighorn Basin (Wyoming, USA). Basin Res. 26, 403–435.

Beaudoin, N., Lacombe, O., Roberts, N.M.W., Koehn, D., 2018. U-Pb dating of calcite veins reveals complex stress evolution and thrust sequence in the Bighorn Basin. Wyoming, USA. Geology 46, 1015–1018.

Bitzer, K., Travé, A., Carmona, J.M., 2001. Fluid flow processes at basin scale. Acta Geol. Hisp. 36, 1–20.

Burisch, M., Gerdes, A., Walter, B.F., Neumann, U., Fettel, M., Markl, G., 2017. Methane and the origin of five-element veins: mineralogy, age, fluid inclusion chemistry and ore forming processes in the Odenwald, SW Germany. Ore Geol. Rev. 81, 42–61.

Capelli, I.A., Scasso, R.A., Kietzman, D.A., Cravero, F., Minisini, D., Catalano, J.P., 2018. Mineralogical and geochemical trends of the Vaca muerta-quintuco system in the Puerta Curaco section, Neuquén basin. Rev. Asoc. Geol. Argent. 75, 210–228.

Carbone, O., Franzese, J., Limeres, M., Delpino, D., Martínez, R., 2011. El Ciclo Precuyano (Triásico Tardío-Jurásico Temprano) en la Cuenca Neuquina. In: Leanza, H., Arregui, C., Carbone, O., Danieli, J.C., Vallés, J.M. (Eds.), Relatorio del XVIII Congreso Geológico Argentino. Asociación Geológica Argentina, Neuquén, pp. 63–76.

Cervera, M., Leanza, H.A., 2009. Hallazgo de sedimentitas sinorogénicas neógenas en los alrededores de Chos Malal, Cuanca Neuquina, Argentina. Rev 11, 14–22.

Chen, Y.W., Wu, J., Suppe, J., 2019. Southward propagation of Nazca subduction along the Andes. Nature 565, 441–447.

Cobbold, P.R., Rodrigues, N., 2007. Seepage forces, important factors in the formation of horizontal hydraulic fractures and bedding-parallel fibrous veins ('beef' and 'cone-in-cone'). Geofluids 7, 313–322.

Cobbold, P.R., Rossello, E.A., 2003. Aptian to recent compressional deformation, foothills of the Neuquén Basin, Argentina. Mar. Petrol. Geol. 20, 429–443.

Cobbold, P.R., Diraison, M., Rossello, E.A., 1999. Bitumen veins and Eocene transpression, Neuquén basin, Argentina. Tectonophysics 314, 423–442.

Cobbold, P.R., Zanella, A., Rodrigues, N., Løseth, H., 2013. Bedding-parallel fibrous veins (beef and cone-in-cone): worldwide occurrence and possible significance in terms of fluid overpressure, hydrocarbon generation and mineralization. Mar. Petrol. Geol. 43, 1–20.

Cobbold, P.R., Ruffet, G., Leith, L., Loseth, H., Rodrigues, N., Leanza, H.A., Zanella, A., 2014. Radial patterns of bitumen dykes around Quaternary volcanoes, provinces of northern Neuquén and southernmost Mendoza, Argentina. J. S. Am. Earth Sci. 56, 454–467.

Colavitto, B., Sagripanti, L., Fennell, L., Folguera, A., Costa, C., 2019. Evidence of Quaternary tectonics along Río Grande valley, southern Malargüe fold and thrust belt, Mendoza, Argentina. Geomorphology 346, 106812.

Cosgrove, J.W., 2015. The association of folds and fractures and the link between folding, fracturing and fluid flow during the evolution of a fold–thrust belt: a brief review. Geological Society, London, Special Publications 421, SP421.

Cruset, D., Vergés, J., Albert, R., Gerdes, A., Benedicto, A., Cantarero, I., Travé, A., 2020. Quantifying deformation processes in the SE Pyrenees using U-Pb dating of fracture-filling calcites. J. Geol. Soc. 177, 1186–1196.

Cruz, C.E., Villar, H.J., Muñoz, G.N., 1996. Los sistemas petroleros del Grupo Mendoza en la fosa de Chos Malal. Cuenca Neuquina, Argentina, XIII. Congreso Geológico Argentino y III Congreso de Exploración de Hidrocarburos, Buenos Aires, Actas, pp. 45–60.

Delvaux, D., Sperner, B., 2003. New aspects of tectonic stress inversion with reference to the TENSOR program. In: Nieuwland, D.A. (Ed.), New Insights into Structural Interpretation and Modelling. Geological Society, London, Special Publications, pp. 75–100.

Domínguez, R.F., Leanza, H.A., Fantín, M., Marchal, D., Cristallini, E., 2020. Basin confifuration during the Vaca Muerta times. In: Minisini, D., Fantín, M., Launusse-Noguera, I., Leanza, H.A. (Eds.), Integrated Geology of Unconventionals: the Case of the Vaca Muerta Play, Argentina. AAPG Memoir, pp. 141–162.

Drake, R.E., 1976. Chronology of cenozoic igneous and tectonic events in the central Chilean Andes — latitudes 35° 30′ to 36°S. J. Volcanol. Geoth. Res. 1, 265–284.

Durney, D.W., Ramsay, J.G., 1973. Incremental strains measured by syntectonic crystal growths. In: De Jong, K.A., Scholten, R. (Eds.), Gravity and Tectonics. Wiley, New York, pp. 67–96.

Eberli, G.P., Weger, R.J., Tenaglia, M., Rueda, L., Rodriguez, L., Zeller, M., McNeill, D.F., Murray, S., Swart, P.K., 2017. The unconventional play in the Neuquén basin, Argentina–insights from the outcrop for the subsurface. In: Unconventional Resources Technology Conference. Society of Exploration Geophysicists, American Association of Petroleum Geologists, Society of Petroleum Engineers, Austin, Texas, pp. 2208–2219.

Fall, A., Ukar, E., López, R.G., Gale, J., Manceda, R., Laubach, S.E., 2017. Timing of opening and cementation of bedding-parallel and vertical fractures. In: Vaca Muerta Formation. Argentina, AAPG Annual Convention and Exhibition, Houston, Texas.

Fennell, L.M., Iannelli, S.B., Encinas, A., Naipauer, M., Valencia, V., Folguera, A., 2019. Alternating contraction and extension in the southern central Andes (35°–37°S). Am. J. Sci. 319, 381.

Fernández, M., Verzi, L.H., Sánchez, E., 2003. Actividad tectonica y evolucion sedimentaria de los depósitos tithoniano-Valanginiano temprano, porcion oriental de la Cuenca Neuquina-Argentina, 8° Simposio Bolivariano - Exploración Petrolera en la Cuencas Subandinas, pp. 233–246.

Folguera, A., Ramos, V.A., Zapata, T., Spagnuolo, M., Miranda, F., 2005. Pliocene to Quaternary retro-arc extension in the Andes at 35° - 37°30′s. In: 6th International Symposium on Andean Geodynamics (ISAG 2005, B., Extended Abstracts, pp. 277–280.

Folguera, A., Ramos, V.A., Zapata, T., Spagnuolo, M.G., 2007. Andean evolution at the Guañacos and Chos Malal fold and thrust belts (36°30′–37°s). J. Geodyn. 44, 129–148.

Folguera, A., Vera, E.R., Bottesi, G., Zamora-Valcarce, G., Ramos, V.A., 2010. The Loncopué trough: a cenozoic basin produced by extension in the southern central Andes. J. Geodyn. 49, 287–295.

Folguera, A., Bottesi, G., Duddy, I., Martín-González, F., Orts, D., Sagripanti, L., Vera, E. R., Ramos, V.A., 2015. Exhumation of the Neuquén Basin in the southern Central Andes (Malargüe fold and thrust belt) from field data and low-temperature thermochronology. J. S. Am. Earth Sci. 64, 381–398.

Franchini, M., López-Escobar, L., Schalamuk, I.B.A., Meinert, L., 2003. Magmatic characteristics of the paleocene Cerro nevazón region and other late cretaceous to early tertiary calc-alkaline subvolcanic to plutonic units in the Neuquén Andes, Argentina. J. S. Am. Earth Sci. 16, 399–421.

Galland, O., Hallot, E., Cobbold, P.R., Ruffet, G., d'Ars, J.d.B., 2007. Volcanism in a compressional Andean setting: a structural and geochronological study of Tromen volcano (Neuquén province, Argentina). Tectonics 26.

Garrido, A.C., 2011. El Grupo Neuquén (Cretácico Tardío) en la Cuenca Neuquina. In: Leanza, H., Arregui, C., Carbone, O., Danieli, J.C., Vallés, J.M. (Eds.), Relatorio del XVIII Congreso Geológico Argentino. Asociación Geológica Argentina, Neuquén, pp. 231–244.

Ge, S., Garven, G., 1989. Tectonically induced transient groundwater flow in foreland basin. In: Price, R.A. (Ed.), Origin and Evolution of Sedimentary Basins and Their Energy and Mineral Resources. American Geophysical Union, pp. 145–157.

Gerdes, A., Zeh, A., 2006. Combined U–Pb and Hf isotope LA-(MC-)ICP-MS analyses of detrital zircons: comparison with SHRIMP and new constraints for the provenance and age of an Armorican metasediment in Central Germany. Earth Planet Sci. Lett. 249, 47–61.

Gerdes, A., Zeh, A., 2009. Zircon formation versus zircon alteration – new insights from combined U-Pb and Lu-Hf in-situ La-ICP-MS analyses of Archean zircons from the Limpopo Belt. Chem. Geol. 261, 230–243.

Gianni, G.M., García, H.P.A., Lupari, M., Pesce, A., Folguera, A., 2017. Plume overriding triggers shallow subduction and orogeny in the southern Central Andes. Gondwana Res. 49, 387–395.

Gianni, G.M., Dávila, F.M., Echaurren, A., Fennell, L., Tobal, J., Navarrete, C., Quezada, P., Folguera, A., Giménez, M., 2018. A geodynamic model linking Cretaceous orogeny, arc migration, foreland dynamic subsidence and marine ingression in southern South America. Earth Sci. Rev. 185, 437–462.

González-Estebenet, M.C., Naipauer, M., Pazos, P.J., Valencia, V.A., 2021. U–Pb detrital zircon ages in the Lajas Formation at Portada Covunco: maximum depositional age and provenance implications for the Neuquén Basin, Argentina. J. S. Am. Earth Sci. 110, 103325.

González-Ferrán, O., 1995. Volcanes de Chile. Instituto Geográfico Militar, p. 640.

González-Tomassini, F.G., Fantín, M., Desjardins, P., Vallejo, M.D., Kietzmann, D., Marchal, D., Leanza, H., González, G., Sattler, F., Rivarola, L.G., Domínguez, R.F., Reijenstein, H., Lohler, G., Santiago, M., Jait, D., Minisini, D., Aguirre-Urreta, B., Bande, A., Simó, T., Vittore, F., Crousse, L., Schelotto, M.L.R., Aguirre, H., Feinstein, E., Liberman, A., Cuervo, S., Depine, G., Sylwan, C., Guerberoff, D., Cal, H. D.l., Alonso, S., Suriano, J., Ambrosio, A., Noguera, I.L., 2016. Co-opetition": a game-changing synergy among operators. In: A Case Delivering a Rosetta Stone for the Vaca Muerta Stratigraphy (Argentina), Unconvencional Resources Technology Conference, 1-3 August, San Antonio, Texas, USA.

Gulisano, C., 1981. El Ciclo Cuyano en el norte del Neuquén y sur de Mendoza. 8th Congreso Geológico Argentino. Actas 3, 579–592 (San Luis).

Gulisano, C.A., Gutiérrez-Pliemling, A.-R., 1995. Guía de campo: el Jurásico de la Cuenca Neuquina b) Provincia de Mendoza. In: Asociación Geológica de Argentina Serie E, pp. 1–111.

Gutiérrez-Pleimling, A., Olea, G., Suárez, M., Valenzuela, M., 2011. El miembro chorreado de la Formación Huitrín (cretácico temprano). In: Leanza, H., Arregui, C., Carbone, O., Danieli, J.C., Vallés, J.M. (Eds.), Relatorio del XVIII Congreso Geológico Argentino. Asociación Geológica Argentina, Neuquén, pp. 175–180.

Guzmán, C., Cristallini, E., Bottesi, G., 2007. Contemporary stress orientations in the Andean retroarc between 34°S and 39°S from borehole breakout analysis. Tectonics 26.

Hansman, R.J., Albert, R., Gerdes, A., Ring, U., 2018. Absolute ages of multiple generations of brittle structures by U-Pb dating of calcite. Geology 46, 207–210.

Hervé, F., Calderón, M., Fanning, C.M., Pankhurst, R.J., Godoy, E., 2013. Provenance variations in the Late Paleozoic accrerionary complex of central Chile as indicated by detrital zircons. Gondwana Res. 23, 1122–1135.

Hildreth, W., Fierstein, J., Godoy, E., Drake, R.E., Singer, B., 1999. The puelche volcanic field: extensive pleistocene rhyolite lava flows in the Andes of central Chile. Rev. Geol. Chile 26, 275–309.

Horstwood, M.S.A., Košler, J., Gehrels, G., Jackson, S.E., McLean, N.M., Paton, C., Pearson, N.J., Sircombe, K., Sylvester, P., Vermeesch, P., Bowring, J.F., Condon, D.J., Schoene, B., 2016. Community-Derived standards for LA-ICP-MS U-(Th-)Pb geochronology – uncertainty propagation, age interpretation and data reporting. Geostand. Geoanal. Res. 40, 311–332.

Horton, B.K., 2018. Tectonic regimes of the central and southern Andes: responses to variations in plate coupling during subduction. Tectonics 37, 402–429.

Horton, B.K., Fuentes, F., Boll, A., Starck, D., Ramirez, S.G., Stockli, D.F., 2016. Andean stratigraphic record of the transition from backarc extension to orogenic shortening: a case study from the northern Neuquén Basin, Argentina. J. S. Am. Earth Sci. 71, 17–40.

Howell, J.A., Schwarz, E., Spalletti, L.A., Veiga, G.D., 2005. The Neuquén basin: an overview. In: Veiga, G.D., Spalletti, L.A., Howell, J.A., Schwarz, E. (Eds.), The Neuquén Basin, Argentina: A Case Study in Sequence Stratigraphy and Basin Dynamics, pp. 1–14.

Iannelli, S.B., Litvak, V.D., Fernández-Paz, L., Folguera, A., Ramos, M.M.E., Ramos, V.A., 2017. Evolution of Eocene to Oligocene arc-related volcanism in the north patagonian Andes (39–41°S), prior to the break-up of the Farallon plate. Tectonophysics 696–697, 70–87.

Iglesia Llanos, M.P., Kietzmann, D.A., Martinez, K., Palma, R.M., 2017. Magnetostratigraphy of the upper jurassic–lower cretaceous from Argentina: implications for the J-K boundary in the Neuquén basin. Cretac. Res. 70, 189–208.

Jessell, M.W., Willman, C.E., Gray, D.R., 1994. Bedding parallel veins and their relationship to folding. J. Struct. Geol. 16, 753–767.

Jordan, T.E., Burns, W.M., Veiga, R., Pángaro, F., Copeland, P., Kelley, S., Mpodozis, C., 2001. Extension and basin formation in the southern Andes caused by increased convergence rate: a mid-Cenozoic trigger for the Andes. Tectonics 20, 308–324.

Karg, H., Littke, R., 2020. Tectonic control on hydrocarbon generation in the northwestern Neuquén Basin, Argentina. AAPG (Am. Assoc. Pet. Geol.) Bull. 104, 2173–2208.

Kietzmann, D.A., Palma, R.M., Llanos, M.P.I., 2015. Cyclostratigraphy of an orbitally-driven tithonian–valanginian carbonate ramp succession, southern Mendoza, Argentina: implications for the jurassic–cretaceous boundary in the Neuquén basin. Sediment. Geol. 315, 29–46.

Kietzmann, D.A., Ambrosio, A.L., Suriano, J., ALonso, M.S., Tomassini, F.G., Depine, G., Repol, D., 2016. The Vaca muerta–quintuco system (Tithonian–Valanginian) in the Neuquén basin, Argentina: a view from the outcrops in the Chos Malal fold and thrust belt. AAPG (Am. Assoc. Pet. Geol.) Bull. 100, 743–771.

Kozlowski, E.E., Cruz, C.E., Sylwan, C.A., 1997. Modelo exploratorio en la faja corrida de la Cuenca Neuquina, Argentina, Asociación Colombiana de Geología del Petroleo, Bogotá. VI Simposio Bolivariano, Memorias, pp. 15–31.

Kozlowski, E.E., Cruz, C.E., Sylwan, C.A., 1998. Modelo exploratorio en la faja corrida de la Cuenca Neuquina, Argentina, 55. Boletín de Informaciones Petroleras, pp. 4–23.

Krim, N., Bonnel, C., Tribovillard, N., Imbert, P., Aubourg, C., Riboulleau, A., Bout-Roumazeilles, V., Hoareau, G., Fasentieux, B., 2017. Paleoenvironmental evolution of the southern neuquèn basin (Argentina) during the tithonian-berriasian (Vaca Muerta and picún Leufú formations): a multi-proxy approach. Bull. Soc. Geol. Fr. 188, 34.

Krim, N., Tribovillard, N., Riboulleau, A., Bout-Roumazeilles, V., Bonnel, C., Imbert, P., Aubourg, C., Hoareau, G., Fasentieux, B., 2019. Reconstruction of palaeoenvironmental conditions of the Vaca Muerta formation in the southern part of the Neuquén Basin (Tithonian-Valanginian): evidences of initial short-lived development of anoxia. Mar. Petrol. Geol. 103, 176–201.

Larmier, S., 2020. Génération de fluides, migration et fracturation au sein des roches mères : cas de la formation de la Vaca Muerta, bassin de Neuquén, Argentine. PhD thesis. Le Mans Université, Le Mans, France, p. 488.

Larmier, S., Zanella, A., Lejay, A., Mourgues, R., Gelin, F., 2021. Geological parameters controlling the bedding-parallel vein distribution in Vaca Muerta Formation core data, Neuquén Basin, Argentina. AAPG (Am. Assoc. Pet. Geol.) Bull. https://doi.org/10.1306/03122119201.

Leanza, H.A., 2003. Las sedimentitas huitrinianas y rayosianas (Cretácico Inferior) en el ámbito central y meridional de la Cuenca Neuquina, Argentina, vol. 2. SEGEMAR, Serie de Contribuciones Téctinas, Geología, pp. 1–31.

Leanza, H.A., Hugo, C.A., 1997. Hoja Geológica 3969-III, Picún Leufú, provincias del Nequén y Río Negro. Programa Nacional de Cartas Geológicas de la República Argentina a escala 1:250000. Insituto de Geología y Recursos Minerales. SEGE-MAR. Boletín 218, 1–135.

Leanza, H.A., Marchese, H.G., Riggi, J.C., 1977. Estratigrafía del Grupo Mendoza con especial referencia a la Formación Vaca Muerta entre los Paralelos 35° y 40° l.s. Cuenca Neuquina-Mendocina. Rev. Asoc. Geol. Argent. 32, 190–208.

Leanza, H.A., Sattler, F., Martínez, R., Carbone, O., 2011a. La Formación Vaca Muerta y Equivalentes (Jurásico Tardío – cretácico Temprano) en la Cuenca Neuquina. In: Leanza, H.A., Arregui, C., Carbone, O., Daniela, J.C., Vallés, J.M. (Eds.), Geología y Recursos Naturales de la Provincia del Neuquén, pp. 113–129. Neuquén.

Leanza, H.A., Sattler, F., Martínez, R.S., Carbone, O., 2011b. La Formación Vaca Muerta y equivalentes (Jurásico Tardío-Cretácico Temprano) en la Cuenca Neuquina. In: Leanza, H., Arregui, C., Carbone, O., Danieli, J.C., Vallés, J.M. (Eds.), Relatorio del XVIII Congreso Geológico Argentino. Asociación Geológica Argentina, Neuquén, pp. 113–129.

Lebinson, F., Turienzo, M., Sánchez, N., Araujo, V., D'Annunzio, M.C., Dimieri, L., 2018. The structure of the northern Agrio fold and thrust belt (37°30' S), Neuquén Basin, Argentina. Andean Geol. 45, 249–273.

Legarreta, L., Gulisano, C.A., 1989. Análisis estratigráfico secuencial de la Cuenca neuquina (triásico superior-terciario). In: Chebli, G., Spalletti, L. (Eds.), Cuencas Sedimentarias Argentinas, Correlación Geológica. Serie, pp. 221–243.

Lesta, P.J., Digregorio, J., Mozetic, M.A., 1985. Presente y futuro de la exploración de petróleo en las cuencas subandinas, Argentina, II Simposio Bolivariano. Exploración Petrolera en las Cuencas Subandinas, Bogotá, pp. 1–35.

Linnemann, U., Ovtcharova, M., Schaltegger, U., Gärtner, A., Hautmann, M., Geyer, G., Vickers-Rich, P., Rich, T., Plessen, B., Hofmann, M., Zieger, J., Krause, R., Kriesfeld, L., Smith, J., 2018. New high-resolution age data from the Ediacaran–Cambrian boundary indicate rapid, ecologically driven onset of the Cambrian explosion. Terra. Nova 31, 49–58.

Llambías, E.J., Rapela, C.W., 1989. Las volcanitas de Collipilli, Neuquén (37°S) y su relación con otras unidades Paleógenas de la cordillera. Rev. Asoc. Geol. Argent. 44, 224–236.

Ludwig, K.R., 2012. User's Manual for Isoplot Version 3.75: A Geochronological Toolkit for Microsoft Excel, vol. 5. Berkeley Geochronology Center Special Publication.

Machel, H.G., Cavell, P.A., 1999. Low-flux, tectonically-induced squeegee fluid flow ("hot flash") into the Rocky Mountain Foreland Basin. Bull. Can. Petrol. Geol. 47, 510–533.

Manceda, R., Figueroa, D., 1995. Inversion of the mesozoic Neuquén rift in the Malargüe fold and thrust belt, Mendoza, argentin. In: Tankard, A.J., Soruco, R.S., Welsink, H.J. (Eds.), Petroleum Basins of South America. American Association of Petroleum Geologists, pp. 369–382.

Mangenot, X., Gasparrini, M., Gerdes, A., Boniface, M., Rouchon, V., 2018. An emerging thermochronometer for carbonate-bearing rocks D47/(U-Pb). Geology 46, 1067–1070.

Martínez, K., Kietzmann, D.A., Llanos, M.P.I., Leanza, H.A., Luppo, T., 2018. Magnetostratigraphy and cyclostratigraphy of the tithonian interval from the Vaca Muerta formation, southern Neuquén basin, Argentina. J. S. Am. Earth Sci. 85, 209–228.

Messager, G., Nivière, B., Martinod, J., Lacan, P., Xavier, J.P., 2010. Geomorphic evidence for plio-quaternary compression in the andean foothills of the southern Neuquén basin, Argentina. Tectonics 29, TC4003.

Mosquera, A., Ramos, V.A., 2006. Intraplate deformation in the Neuquén embayment. In: Kay, S.M., Ramos, V.A. (Eds.), Evolution of an Andean Margin: A Tectonic and Magmatic View from the Andes to the Neuquén Basin (35°–39°S Lat). Geological Society of America Special Paper, pp. 97–123.

Mpodozis, C., Ramos, V.A., 1989. The Andes of Chile and Argentina. In: Eriksen, G.E., Cañas-Pinochet, M.T., Reinemud, J.A. (Eds.), Geology of the Andes and its' Relation to Hydrocarbon and Mineral Resources. Circumpacific Council for Energy and Mineral Resources, Earth Sciences Series, Houston, pp. 59–90.

Munizaga, F., Huete, C., Hervé, F., 1985. Geocronología K-Ar y razones iniciales Sr87/Sr86 de la "Faja Pacífica" de "Desarrollos hidrotermales. 4° Congreso Geológico Chileno (Antofagasta), Actas 3, 357–379.

Naipauer, M., García-Morabito, E., Marques, J.C., Tunik, M., Vera, E.A.R., Vujovich, G.I., Pimentel, M.P., Ramos, V.A., 2012. Intraplate Late Jurassic deformation and exhumation in western central Argentina: constraints from surface data and U–Pb detrital zircon ages. Tectonophysics 524–525, 59–75.

Nuriel, P., Weinberger, R., Kylander-Clark, A.R.C., Hacker, B.R., Craddock, J.P., 2017. The onset of the Dead Sea transform based on calcite age-strain analyses. Geology 45, 587–590.

Nuriel, P., Wotzlaw, J.F., Ovtcharova, M., Vaks, A., Stremtan, C., Šala, M., Roberts, N.M. W., Kylander-Clark, A.R.C., 2021. The use of ASH-15 flowstone as a matrix-matched reference material for laser-ablation U − Pb geochronology of calcite. Geochronology 3, 35–47.

Pagel, M., Bonifacie, M., Schneider, D.A., Gautheron, C., Brigaud, B., Calmels, D., Cros, A., Saint-Bezar, B., Landrein, P., Sutcliffe, C., Davis, D., Chaduteau, C., 2018. Improving paleohydrological and diagenetic reconstructions in calcite veins and breccia of a sedimentary basin by combining Δ47 temperature, δ18Owater and U-Pb age. Chem. Geol. 481, 1–17.

Pardo-Casas, F., Molnar, P., 1987. Relative motion of the Nazca (Farallon) and south American plates since late cretaceous time. Tectonics 6, 233–248.
Parnell, J., Carey, P.F., 1995. Emplacement of bitumen (asphaltite) veins in the Neuquén Basin, Argentina. AAPG (Am. Assoc. Pet. Geol.) Bull. 79, 1798–1816.
Passchier, C.W., Trouw, R.A.J., 2005. Microtectonics, 2 ed. Springer Berlin Heidelberg.
Radic, J.P., Rojas, L., Carpinelli, A., Zurita, E., 2002. Evolución tectónica de la cuenca Terciaria de Cura-Mallín Región Cordillerana Chileno Argentina (36°30'-39°00'S). XIV Congreso Geológico Argentino (Calafate), Actas 3, 233–237.
Ramos, V.A., 1978. Estructura. Relatorio de la geología y recursos naturales del Neuquén: Buenos Aires. VII Congreso Geológico Argentino, pp. 99–118.
Ramos, V.A., 1981. Descripción geológica de la Hoja 33c, Los Chihuidos Norte, Provincia del Neuquén, 182. Servicio Geológico Nacional, Buenos Aires, Boletín, pp. 1–103.
Ramos, V.A., 1998. Estructura del sector Occidental de la faja plegada y corrida del Agrio, cuenca Neuquina. Congreso Latinoamericano de Geología, Argentina.
Ramos, V.A., Barbieri, M., 1989. El volcanismo Cenozoico de Huantraico: edad y relaciones isotópicas iniciales, provincia del Neuquén. Rev. Asoc. Geol. Argent. 43, 210–223.
Ramos, V.A., Folguera, A., 2005. Tectonic evolution of the Andes of Neuquén: constraints derived from the magmatic arc and foreland deformation. In: Veiga, G.D., Spalletti, L.A., Howell, J.A., Schwarz, E. (Eds.), The Neuquén Basin, Argentina: A Case Study in Sequence Stratigraphy and Basin Dynamics. Geological Society, London, Special Publications, pp. 15–35.
Ramos, V.A., Litvak, V.D., Folguera, A., Spagnuolo, M., 2014. An Andean tectonic cycle: from crustal thickening to extension in a thin crust (34°–37°SL). Geoscience Frontiers 5, 351–367.
Ravier, E., Martinez, M., Pellenard, P., Zanella, A., Tupinier, L., 2020. The milankovitch fingerprint on the distribution and thickness of bedding-parallel veins (beef) in source rocks. Mar. Petrol. Geol. 122, 104643.
Riccardi, A.C., Leanza, H.A., Damborenea, S.E., Manceñido, M.O., Ballent, S.C., Zeiss, A., 2000. Marine mesozoic biostratigraphy of the Neuquén Basin. Zeitschrift für Angewandte Geologie, Sonderheft 1, 103–108.
Ring, U., Gerdes, A., 2016. Kinematics of the alpenrhein-bodensee graben system in the central alps: oligocene/miocene transtension due to Formation of the western alps arc. Tectonics 35, 1367–1391.
Roberts, N.M.W., Walker, R.J., 2016. U-Pb geochronology of calcite-mineralized faults: absolute timing of rift-related fault events on the northeast Atlantic margin. Geology 44, 531–534.
Roberts, N.M.W., Rasbury, E.T., Parrish, R.R., Smith, C.J., Horstwood, M.S.A., Condon, D.J., 2017. A calcite reference material for LA-ICP-MS U-Pb geochronology. G-cubed 18, 2807–2814.
Rochelle-Bates, N., Roberts, N.M.W., Sharp, I., Freitag, U., Verwer, K., Halton, A., Fiordalisi, E., Dongen, B.E.v., Swart, R., Ferreira, C.H., Dixon, R., Schröder, S., 2020. Geochronology of volcanically associated hydrocarbon charge in the pre-salt carbonates of the Namibe Basin, Angola. Geology 49, 335–340.
Rodrigues, N., Cobbold, P.R., Loseth, H., Ruffet, G., 2009. Widespread bedding-parallel veins of fibrous calcite ('beef') in a mature source rock (Vaca Muerta Fm, Neuque'n Basin, Argentina): evidence for overpressure and horizontal compression. J. Geol. Soc. 166, 695–709.
Rodríguez, M.F., 2011. El Grupo Malargüe (Cretácico Tardío-Paleógeno temprano) en la Cuenca Neuquina. In: Leanza, H., Arregui, C., Carbone, O., Danieli, J.C., Vallés, J.M. (Eds.), Relatorio del XVIII Congreso Argentino. Asociación Geológica Argentina, Neuquén, pp. 245–264.
Rojas Vera, E.A.R., Folguera, A., Valcarce, G.Z., Bottesi, G., Ramos, V.A., 2014. Structure and development of the Andean system between 36° and 39°S. J. Geodyn. 73, 34–52.
Rojas Vera, E.A.R., Mescua, J., Folguera, A., Becker, T.P., Sagripanti, L., Fennell, L., Orts, D., Ramos, V.A., 2015. Evolution of the Chos Malal and Agrio fold and thrust belts, Andes of Neuquén: insights from structural analysis and apatite fission track dating. J. S. Am. Earth Sci. 64, 418–433.
Roure, F., Swennen, R., Schneider, F., Faure, J.L., Ferket, H., Guilhaumou, N., Osadetz, K., Robion, P., Vandeginste, V., 2005. Incidence and importance of tectonics and natural fluid migration on reservoir evolution in foreland fold-and-thrust belts. Oil Gas Sci. Technol. 60, 67–106.
Sagripanti, L., Bottesi, G., Kietzmann, D., Folguera, A., Ramos, V.A., 2012. Mountain building processes at the orogenic front. A study of the unroofing in Neogene foreland sequence (37°S). Andean Geol. 39, 201–219.
Sagripanti, L., Rojas-Vera, E.A., Gianni, M.G., Folguera, A., Harvey, J.E., Farías, M., Ramos, V.A., 2015. Neotectonic reactivation of the western section of the Malargüe fold and thrust belt (Tromen volcanic plateau, Southern Central Andes). Geomorphology 232, 164–181.
Sagripanti, L., Folguera, A., Fennell, L., Rojas-Vera, E.A., Ramos, V.A., 2016. Progression of the deformation in the southern central Andes (37°S). In: Folguera, A., Naipauer, M., Sagripanti, L., Chiglione, M., Orts, D., Giambiagi, L. (Eds.), Growth of the Southern Andes. Springer Earth System Sciences, pp. 115–132.
Sánchez, N.P., Coutand, I., Turienzo, M., Lebison, F., Araujo, V., Dimieri, L., 2018. Tectonic evolution of the Chos Malal fold-and-thrust belt (Neuquén Basin, Argentina) from (U-Th)/He and fission track thermochronometry. Tectonics 37.
Scasso, R.A., Alonso, M.S., Lanés, S., Villar, H.J., Laffitte, G., 2005. Geochemistry and petrology of a Middle Tithonian limestone-marl rhythmite in the Neuquén Basin, Argentina: depositional and burial history. Geological Society 252, 207–229. London, Special Publications.
Scheuber, E., Bogdanic, T., Jensen, A., Reutter, K.J., 1994. Tectonic development of the North Chilean Andes in relation to plate convergence and magmatism since the Jurassic. In: Reutter, K.J., Scheuber, E., Wigger, P.J. (Eds.), Tectonics of the Southern Central Andes: Structure and Evolution of an Active Continental Margin. Springer-Verlag, Berlin, pp. 121–139.
Schwarz, E., Spalletti, L.A., Howell, J.A., 2006. Sedimentary response to a tectonically induced sea-level fall in a shallow back-arc basin: the Mulichinco Formation (Lower Cretaceous), Neuquén Basin, Argentina. Sedimentology 53, 55–81.
Schwarz, E., Spalletti, L.A., Veiga, G.D., 2011. La Formación Mulichinco (Cretácico Tardío) en la Cuenca Neuquina. In: Leanza, H., Arregui, C., Carbone, O., Danieli, J. C., Vallés, J.M. (Eds.), Relatorio del XVIII Congreso Geológico Argentino. Asociación Geológica Argentina, Neuquén, pp. 131–144.
Somoza, R., Ghidella, M.E., 2012. Late Cretaceous to recent plate motions in western South America revisited. Earth Planet Sci. Lett. 331–332, 152–153.
Spalletti, L.A., Veiga, G.D., Schwarz, E., Franzese, J., 2008. Depósitos de flujos gravitacionales subácueos de sedimentos en el flanco activo de la cuenca neuquina durante el Cretácico temprano. Rev. Asoc. Geol. Argent. 63, 442–453.
Spalletti, L.A., Arregui, C.D., Veiga, G.D., 2011a. La Formación Tordillo y equivalentes (Jurásico Tardío) en la Cuenca Neuquina. In: Leanza, H., Arregui, C., Carbone, O., Danieli, J.C., Vallés, J.M. (Eds.), Relatorio del XVIII Congreso Geológico Argentino. Asociación Geológica Argentina, Neuquén, pp. 99–111.
Spalletti, L.A., Veiga, G.D., Schwarz, E., 2011b. La Formación Agrio (Cretácico Temprano) en la Cuenca Neuquina. In: Leanza, H., Arregui, C., Carbone, O., Danieli, J.C., Vallés, J.M. (Eds.), Relatorio del XVIII Congreso Argentino. Asociación Geológica Argentina, Neuquén, pp. 145–160.
Steinmann, G., 1929. Geologie von Perú.
Stinco, L.P., Mosquera, A., 2003. Estimación del contenido total de carbono orgánico a partir de registros de pozo para las Formaciones Vaca Muerta y Los Molles, Cuenca Neuquina, Argentina, p17. II° Congreso de hidrocarburos, IAPG, Actas-CD-ROM, Buenos Aires.
Stipanicic, P.N., Rodrigo, F., Baulies, O.L., Martínez, C.G., 1968. Las formaciones presenonianas en el denominado Macizo Nordpatagonico y areas adyacentes. Rev. Asoc. Geol. Argent. 23, 67–98.
Stoneley, R., 1983. Fibrous calcite veins, overpressures, and primary oil Migration1. AAPG (Am. Assoc. Pet. Geol.) Bull. 67, 1427–1428.
Tavani, S., Storti, F., Lacombe, O., Corradetti, A., Muñoz, J.A., Mazzoli, S., 2015. A review of deformation pattern templates in foreland basin systems and fold-and-thrust-belts: implications for the state of stress in the frontal regions of thrust wedges. Earth Sci. Rev. 141, 82–104.
Travé, A., Labaume, P., Calvet, F., Soler, A., 1997. Sediment dewatering and pore fluid migration along thrust faults in a foreland basin inferred from isotopic and elemental geochemical analyses (Eocene southern Pyrenees, Spain). Tectonophysics 282, 375–398.
Tunik, M., Folguera, A., Naipauer, M., Pimentel, M., Ramos, V.A., 2010. Early uplift and orogenic deformation in the Neuquén Basin: constraints on the Andean uplift from U–Pb and Hf isotopic data of detrital zircons. Tectonophysics 489, 258–273.
Ukar, E., López, R.G., Gale, J.F.W., Laubach, S.E., Manceda, R., 2017a. New type of kinematic indicator in bed-parallel veins, late jurassic-early cretaceous Vaca Muerta formation, Argentina: E-W shortening during late cretaceous vein opening. J. Struct. Geol. 104, 31–47.
Ukar, E., López, R.G., Laubach, S.E., Gale, J.F.W., Manceda, R., Marrett, R., 2017b. Microfractures in bed-parallel veins (beef) as predictors of vertical macrofractures in shale: Vaca Muerta Formation, Agrio Fold-and-Thrust Belt, Argentina. J. S. Am. Earth Sci. 79, 152–169.
Ukar, E., Gale, J.F.W., Fall, A., López, R.G., Hryb, D., Manceda, R., Brisson, I., Hernandez-Bilbao, E., Weger, R.J., Marchal, D.A., Zanella, A., Cobbold, P.R., 2020. Natural fractures: from core and outcrop observations to subsurface models. In: Minisini, D., Fantín, M., Noguera, I.L., Leanza, H.A. (Eds.), Integrated Geology of Unconventionals: the Case of the Vaca Muerta Play. AAPG Memoir, Argentina, pp. 377–416.
Urien, C.M., Zambrano, J.J., 1994. Petroleum systems in the Neuquén basin, Argentina. In: Magoon, L.B., Dow, W.G. (Eds.), The Petroleum System—From Source to Trap. American Association of Petroleum Geologists, pp. 513–534.
Veiga, G.D., Spalletti, L.A., 2007. The upper jurassic (kimmeridgian) fluvial–aeolian systems of the southern Neuquén basin, Argentina. Gondwana Res. 11, 286–302.
Veiga, G.D., Schwarz, E., Spalletti, L., 2011. Stratigraphic analysis of the Lotena Formation (upper callovian-lower oxfordian) in central neuquen basin, Argentina. Andean Geol. 38, 171–197.
Weaver, C.E., 1931. Paleontology of the jurassic and cretaceous of west central Argentina. J. Geol. 40, 181–182.
Weger, R.J., Rodríguez-Blanco, L., Eberli, G.P., 2017. A basinal reference section and lateral variability of the Vaca Muerta Formation in the Neuquén Basin. In: Argentina, XX Congreso Geológico Argentino. San Miguel de Tucumán, pp. 179–184, 7-11 August.
Weger, R.J., Murray, S.T., McNeill, D.F., Swart, P.K., Eberli, G.P., Rodríguez-Blanco, L., Tenaglia, M., Rueda, L.E., 2019. Paleothermometry and distribution of calcite beef in the Vaca Muerta Formation, Neuqu'en Basin, Argentina. AAPG (Am. Assoc. Pet. Geol.) Bull. 103, 931–950.
Zamora Valcarce, G.Z., 2007. Estructura y Cinemática de la faja plegada y corrida del Agrio, Cuenca Neuquina (PhD thesis). Universidad de Buenos Aires, Buenos Aires, p. 303.
Zamora Valcarce, G.Z., Pino, D.d., Ansa, A., 2006. Structural evolution and magmatic characteristics of the Agrio fold-and-thrust belt. Geological Society of America 407, 125–145.
Zanella, A., Cobbold, P.R., Le Carlier de Veslud, C., 2014. Physical modelling of chemical compaction, overpressure development, hydraulic fracturing and thrust detachments in organic-rich source rock. Mar. Petrol. Geol. 55, 262–274.
Zanella, A., Cobbold, P.R., Ruffet, G., Leanza, H.A., 2015. Geological evidence for fluid overpressure, hydraulic fracturing and strong heating during maturation and migration of hydrocarbons in Mesozoic rocks of the northern Neuquén Basin, Mendoza Province, Argentina. J. S. Am. Earth Sci. 62, 229–242.

Zanella, A., Cobbold, P.R., Rodrigues, N., Loseth, H., Jolivet, M., Gouttefangeas, F., Chew, D., 2021. Source rocks in foreland basins: a preferential context for the development of natural hydraulic fractures. AAPG (Am. Assoc. Pet. Geol.) Bull. 105 (4), 647–668.

Zapata, T., Folguera, A., 2005. Tectonic evolution of the Andean fold and thrust belt of the southern Neuquén basin, Argentina. In: Spalletti, G.D., Howell, L.A., Schwarz, J. A. (Eds.), The Neuquén Basin, Argentina: A Case Study in Sequence Stratigraphy and Basin Dynamics. Geological Society, London, Special Publications, pp. 37–56.

Zapata, T., Brissón, I., Dzelalija, F., 1999. La estructura de la faja plegada y corrida andina en relación con el control del basamento de la Cuenca Neuquina. Bol. Inf. Pet. (1924) 60, 112–121.

Zavala, C., 1996. High-resolution sequence stratigraphy in the middle jurassic Cuyo group, south Neuquén basin, Argentina. GeoResearch Forum 1–2, 295–304.

Zavala, C., Ponce, J.J., 2011. La Formación Rayoso (Cretácico Temprano) en la Cuenca Neuquina. In: Leanza, H., Arregui, C., Carbone, O., Danieli, J.C., Vallés, J.M. (Eds.), Relatorio del XVIII Congreso Geológico Argentino. Asociación Geológica Argentina, Neuquén, pp. 205–222.

Zeller, M., Eberli, G.P., Weger, R.F., Giunta, D.L., Massaferro, J.L., 2014. Expressions of the Quintuco-Vaca Muerta system based on outcrop facies and geometry, IX Congreso de Exploración y Desarrollo de Hidrocarburos.

Zeller, M., Reid, S.B., Eberli, G.P., Weger, R.J., Massaferro, J.L., 2015. Sequence architecture and heterogeneities of a field – scale Vaca Muerta analog (Neuquén Basin, Argentina) – from outcrop to synthetic seismic. Mar. Petrol. Geol. 66, 829–847.